EXPERIMENTAL AND NUMERICAL ANALYSIS OF AIR CONDITIONING SYSTEM USING MICROCHANNEL HEAT EXCHANGER

PROJECT REPORT

Submitted by

ABHIJITH K R

TKM20MEIR01

to

APJ Abdul Kalam Technological University
in partial fulfilment of the requirements for the award of
Master of Technology in
Industrial Refrigeration and Cryogenic Engineering.
(Mechanical Engineering)

Department of Mechanical Engineering

TKM College of Engineering, Kollam

September 2022

DEPARTMENT OF MECHANICAL ENGINEERING

TKM COLLEGE OF ENGINEERING, KOLLAM

CERTIFICATE

Certified that this report entitled '*Experimental and Numerical Analysis of Air Conditioning System Using Microchannel Heat Exchanger'* is the report of project presented by **ABHIJITH K R, TKM20MEIR01** during **2021-2022** in partial fulfilment of the requirements for the award of the Degree of Master of Technology in Industrial Refrigeration and Cryogenic Engineering, (Mechanical Engineering) of APJ Abdul Kalam Technological University.

Guide:
Dr. Mohammed Sadhikh
Professor
Dept. of Mechanical Engineering
TKM College of Engineering, Kollam

Coordinator:
Dr. Shafi K A
Professor
Dept. of Mechanical Engineering
TKM College of Engineering, Kollam

Dr. Dileep P N
Head of the Department
Dept. of Mechanical Engineering
TKM College of Engineering, Kollam

DECLARATION

I, ABHIJITH K R hereby declare that, this project report entitled **Experimental and Numerical Analysis of Air Conditioning System Using Microchannel Heat Exchanger** is the bonafide work of mine carried out under the supervision of Dr. Mohammed Sadhikh, Professor, Dept. of Mechanical Engineering TKM College of Engineering, Kollam. I declare that, to the best of my knowledge, the work reported here in does not form part of any other project report or dissertation on the basis of which a degree or award was conferred on an earlier occasion to any other candidate. The content of this report is not being presented by any other student to this or any other University for the award of a degree.

ABHIJITH K R
University Register No: TKM20MEIR01 of year 2020-2022

Dr. MOHAMMED SADHIKH
Professor
Dept. of Mechanical Engineering
TKM College of Engineering, Kollam

Dr. DILEEP P N
Professor and Head
Department of Mechanical Engineering
TKM College of Engineering, Kollam

Date:12/09/2022

ACKNOWLEDGEMENT

Any attempt at any level cannot be satisfactorily completed without the support and guidance of learned people. I owe to great many people whose constant support and motivation that has encouraged me to come up with this project. I would like to express my heartfelt thanks to **Dr. Mohammed Sadhikh**, Professor, Department of Mechanical Engineering, TKM College of Engineering for being instrumental in the completion of my project with his guidance.

I express my deep sense of gratitude to **Dr. Dileep P N**, Professor and Head of Department, TKM College of Engineering from bottom of heart for lending me all facilities and support for completion of this project. I thank, **Dr. Shafi K A**, P G Coordinator, Department of Mechanical Engineering, TKM College of Engineering for giving their constant support for doing this project. I would like to thank **Dr. Mohammed Sajid N K,** Professor (Rtd.) and former Head of Department, Department of Mechanical Engineering, TKM College of Engineering for lending me all the facilities and support.

I thank **Dr. Vishnu S B**, Assistant Professor, Department of Mechanical Engineering for his constant support regarding the proceedings of the project. I also extend my regards to instructors: **Mr. Y Johnson, Mr. Viswaraj K V** and tradesmen: **Mr. Nazeer Khan A, Mr. Sooraj A Rasheed** and **Mr. Shahul Hameed S,** Department of Mechanical Engineering for their constant support during the proceedings of my project and I thank other college staffs for the technical and nontechnical assistance given for the project.

I am greatly thankful to **Mr. Suresh T S**, workshop attender, Govt. ITI Vayalar and **Mr. Muhammed Rafeek** for their guidance throughout my project.

I take this opportunity to extend my deep appreciation to family and friends, for all that they meant to me during the crucial times of the completion of this project. Finally, I thank Almighty God for being with me all the time and guiding me with their divine light.

ABHIJITH K R

Place: Kollam

Date: 12/09/2022

ABSTRACT

The potential performance enhancement of a residential split air conditioning system with a microchannel heat exchanger is investigated numerically and verified experimentally. Replacement of fin and tube condenser in the air conditioning system with a microchannel condenser is studied. Numerical analysis of refrigerant flow through microchannel is done and the results shows that the microchannel offers a higher volumetric heat exchange capacity with increased heat transfer area due to the cross section with hydraulic diameter of micrometre range. A residential split air conditioning system of 2 TR cooling capacity with fin and tube condenser and refrigerant R22 is considered for the analysis. The system's numerical and experimental performance analysis is done, and the potential replacement of the fin and tube condenser with a microchannel condenser of the exact dimensions is analysed. The heat duty of the condenser is increased by 82% when the microchannel heat exchanger is installed. Numerical analysis shows that the COP of the system can be improved by 16% by replacing the fin and tube condenser with a microchannel condenser. The microchannel condenser can reduce the overall weight of the outdoor unit since it is compact and 38% lighter than the ordinary bulky fin and tube condenser.

Keywords: Air conditioning system, Microchannel condenser, Heat transfer, Coefficient of Performance (COP), R22.

CONTENTS

LIST OF FIGURES

LIST OF TABLES

ABBREVIATIONS

MCHE	Microchannel Heat Exchanger
HVAC	Heating, Ventilation, and Air Conditioning
RTPF	Round Tube and Plate Fins
CFD	Computational Fluid Dynamics
LP	Low Pressure
HP	High Pressure
RH	Relative Humidity
A/C	Air Conditioning
EER	Energy Efficiency Ratio
COP	Coefficient of Performance
VCRS	Vapour Compression Refrigeration System

NOTATIONS

$\dot{m}$	Mass flow rate [kg/s]
k	Thermal conductivity [W/mK]
ρ	Density [kg/m^3]
ν	Kinematic viscosity [m^2/s]
c_p	Specific heat capacity [kJ/kgK]
h	Specific enthalpy [kJ/kg]
Q	Heat transfer [kW]
$\bar{h}$	Average heat transfer coefficient [W/m^{2}K]
RH	Relative Humidity [%]
Re	Reynolds number
Nu	Nusselt number
Pr	Prandtl number

CHAPTER 1: INTRODUCTION

Heat transfer occupies a central role in a wide range of engineering applications pertaining to energy conversion, encompassing power generation, heating/cooling as well as energy recovery. Thus, heat transfer processes have been the subject of intensive investigations over many years. Forced convection heat exchangers are the widely used heat transfer devices. Here, microchannel heat exchangers (MCHE) have been recently becoming an attractive heat exchanger designs due to their outstanding advantages for certain applications. The most noticeable benefits of the MCHEs are the compact design and improved total heat transfer coefficient (Basaran et al., 2019). The MCHEs are becoming widespread designs in industrial applications like refrigeration, electronic cooling, air--conditioning, heat pump, HVAC, etc, recently. In these applications, the system is designed in a way that the working fluid, generally refrigerant, undergoes a phase change in condenser/evaporator. Achieving a high heat transfer rate in small volumes is one of the main challenges in heat exchanger design, in general. The MCHEs are most promising design to meet this challenge due to their advantages.

Air cooled condensers have attracted wide attention, especially in terms of deficiency of water resources and environmental deterioration. However, the disadvantages of an air-cooled condenser, such as low overall heat transfer coefficient, huge volume, and large pressure drop, limit its extent of application.

1.1 MICROCHANNEL HEAT EXCHANGERS

Microchannel heat exchangers, or micro-structured heat exchangers are heat exchangers in which (at least one) fluid flows in lateral confinements with typical dimensions below 1 mm. The most typical such confinement are microchannels, which are channels with a hydraulic diameter below 1 mm. The concept of microchannel heat exchangers was proposed and used by Tuckerman & Pease in 1981 and the first micro heat exchanger was developed by Swift in 1985.

Recently, the brazed aluminium microchannel heat exchanger has attracted many investigators because it is one possible replacement for the finned-tube heat exchanger. Due to the increasing demand for light weight and rising copper prices, copper substitution is also a widespread concern. The microchannel heat exchanger offers such

significant benefits as compactness, no thermal contact resistance, and small refrigerant charge, compared to the conventional finned round-tube heat exchanger.

1.1.1 Classification of Microchannel

It is a very debatable topic between the researchers to define a definition of microchannel. Mehendale et al. (2000) used a classification technique which is based on manufacturing to obtain various varieties of channel dimensions, where D is the smallest channel dimension.

1 μm < D < 100: Microchannels

100 μm < D < 1 mm: Minichannels

1 mm < D < 6 mm: Compact Passages

6 mm < D: Conventional Passages

Kandlikar and Grande (2003) adopted a different classification based on the rarefaction effect of gases in various ranges of channel dimensions, D being the smallest channel dimension:

1 μm < D < 10 μm: transitional Microchannels

10 μm < D < 200 μm: Micro channels

200 μm < D < 3mm: Mini channels

3mm < D: Conventional Passages

1.1.2 Pros and Cons of Using Smaller Diameter Channels

A high surface area density with small diameter could substantially reduce the volume of heat exchangers needed for the same thermal power. As a result, the space and cost of material associated with construction and installation could be lowered significantly. Moreover, the fluid holdup is slight in a micro heat exchanger, essential for security and economic considering expensive, toxic, or explosive working fluids. The quick response time of microchannels could provide better temperature control for relatively small temperature differences between fluid flows.

Though small diameter channels are advantageous in many ways, they are not without limitations. Because of the petite size of channels, the pressure drop requires high mechanical power for running the system and strict demands for its accessories such as

leak-free connections and pumping devices. Additionally, fine channels are sensitive to corrosion, roughness, and fouling of the surfaces. Channel walls can erode due to chemical etching or the physical wearing out of the inner wall surfaces. For this reason, only very clean fluids could be employed in a microchannel heat sink with protection filters, as mechanical cleaning and maintenance, in general, are not possible. Moreover, specific effects such as fluid maldistribution, axial direction heat conduction, and external losses, which may not be significant in conventional scale heat exchangers, may also be present in small diameter channels.

1.2 MICROCHANNEL CONDENSERS

Microchannel condensers are already used in automobile air conditioning. The advantages of these condensers over the traditional fin-and-tube condensers includes compactness, reduced air side pressure drop, and reduced refrigerant charge, which makes them beneficial in terms of environmental effect in case of a leakage. Compared with a plate-type condenser with a similar heat transfer area, the overall heat transfer coefficient of the microchannel heat exchanger is 62% higher than that of the plate-type condenser, even with 23% less refrigerant (Zhong et al., 2014).

In recent years, microchannel condensation has attracted the attention of some researchers as a new method of strengthening condensation heat transfer. This research aims to discuss possible application of microchannel condenser for a residential air conditioning system.

1.3 OBJECTIVES

The main aim of this project is to carry out the analysis of an air conditioning system using microchannel heat exchanger. This includes the numerical as well as experimental the analysis of a residential split air conditioning system using microchannel condenser. This thesis also includes the numerical analysis flow of refrigerant through a microchannel and the heat transfer associated with it. The objective of this research is as follows:

1. Analyse the heat transfer in microchannels.
2. Conduct numerical simulation of microchannel heat exchanger and study of heat transfer inside the heat exchanger.
3. Validate the simulation results with experiment.

4. Compare the performance of a residential split air conditioning system with normal fin and tube condenser and a microchannel condenser.

1.4 METHODOLOGY

The detailed methodology of the above work is described:

1. **Analysis of Heat Transfer in Microchannels**

   Validation of numerical model with data from literature (Xia and Chan, 2015).

   Simulation of heat transfer between hot fluid and the cold channel surface with CFD package i.e., ANSYS Fluent.

   Simulation of heat transfer with refrigerant- R22.

   Analysis of change in heat transfer by varying the cross section of the microchannel.

2. **Numerical Simulation and Study of Microchannel Heat Exchanger**

   Modelling of microchannel heat exchanger with Solidworks.

   Validation of numerical model with data from literature (Meral and Parlak, 2021).

   Simulation of flow with R22 and analysis of temperature and pressure variation during the flow.

   Mass flow rate is varied to observe the change in outlet temperature.

3. **Performance Comparison of Microchannel Condenser with Fin and Tube Condenser**

   Literature review of microchannel condensers.

   Simulation of flow of refrigerant through the condenser.

   Replacing the fin and tube condenser with microchannel condenser.

   Experimental study and performance analysis.

   Validation of simulation results with the experimental data.

   Comparison of the results.

CHAPTER 2: LITERATURE REVIEW

Due to their performance and portability, heat exchangers with multi-ported microchannel tubes are already utilised in mobile air conditioning systems. According to Xia and Chan (2015), numerous researchers have researched the properties of heat transmission, pressure drop, and flow patterns in order to better understand the physical processes in microchannel tubes.

In addition to their use as condensers in mobile air conditioning systems and as gas coolers in CO2 systems, microchannel heat exchangers may also be utilised as condensers in residential air conditioning systems rather than the more conventional condensers with round tubes. It is well known that RTPF (Round Tubes and Plate Fins) heat exchangers cannot match the compactness of microchannel heat exchangers. Therefore, it can be concluded that for a given heat exchanger package volume, microchannel heat exchangers have a higher capacity than RTPF heat exchangers.

2.1 STUDIES ON MICROCHANNEL FLOW

Using ANSYS CFX 2015, Razali and Sadikin (2015) reported a numerical simulation of flow in a microchannel heat sink. Using published experimental data as validation, the square-shaped model showed superior performance over those with rectangular shapes. Additionally, rather than being rectangular, the square-shaped microchannel exhibited better agreement with values, according to the findings of the pressure-drop test. Based on temperature, pressure, and velocity across the microchannel heat sink, the single flow of microchannel also provided benefits when employing square-shaped microchannel.

A study on the improved heat transfer impact in microsized channels was published in 2015 by Xia and Chen. To examine this micro impact, a simulation model has been developed using the ANSYS Fluent computational fluid dynamics (CFD) platform. It is discovered that the heat transfer rate per unit effective heat transfer area is higher if the inlet area grows smaller as the area of the inlet is varied to examine and identify the enhanced heat absorption resulting from the size effect. If smaller radii channels are taken into account, a lower pressure loss can also be inferred.

In order to examine the properties of heat transmission, Basaran et al. (2019) undertook a series of numerical simulations on the condensing flow of R600a inside a single circular microchannel. This was motivated by the dearth of knowledge on R600a condensation in microchannels. Two-phase flow was modelled using the Volume of Fluid model, and the phase change at saturation temperature was studied using the Lee model. According to observations, the heat transfer coefficient rises as hydraulic diameter decreases and mass flux rises, which is consistent with general findings in the literature for various working fluids. Furthermore, for all simulated diameter and mass flux values, it is seen that an increase in input vapour quality leads to a larger heat transfer coefficient. With an increase in inlet vapour quality, the main causes of this scenario are an increase in vapour core diameter and a decrease in liquid film thickness inside microchannels.

2.2 STUDIES ON MICROCHANNEL CONDENSERS

RTPF heat exchangers offer a cost advantage, which is one of the most important aspects of commercial products, therefore even if microchannel heat exchangers appear to have higher heat transfer properties, they are less frequently employed in home air-conditioning systems. As a result, it was challenging to locate in the open literature the experimental confirmation of the impact of a microchannel condenser on a domestic air-conditioning system.

Experimental research on the prospective use of the microchannel condenser in the domestic air conditioner was conducted by Bea and Han in 1996. In comparison to the fin-and-tube condenser, they claimed that the microchannel heat exchanger may lower the condenser volume by 40% and the charge quantity by 22% while maintaining the same condenser heat transfer rate. They also looked into how the performance of the system was affected by the various numbers of passes the microchannel heat exchanger made. The cooling capacity rose by 4% and the compressor power reduced by 0.9% when the microchannel condenser's pass was adjusted from 4 to 6.

The system performance of the package air conditioner with a microchannel condenser was assessed by Cho et al. in 1999. They claimed that the smaller microchannel condenser, which had 82% less face area than the fin-and-tube condenser, produced the same cooling capacity. Additionally, when the fin pitch is lowered from 3.0 mm to 2.5 mm or 2.0 mm, the refrigerant charge quantity is reduced by 35% and 45%, respectively.

A parallel-flow microchannel tube unit and a round-tube unit were the two types of condensers that were the subject of experimental heat-transfer and pressure-drop measurements made by Park and Hrnjak (2002). The enhanced cooling capability and performance coefficient demonstrated the advantages of the microchannel architecture. In comparison to the system utilising a round-tube condenser, the charge for the system employing a microchannel condenser was 9% lower.

By varying the tube and fin pitches, Jeong et al. (2004) examined the performance of three microchannel condensers with varied air-side heat transfer areas but the same face area (78% of the fin-and-tube condenser). The cooling capacities and COPs approached those of the fin-and-tube condenser system with increases in the heat transfer area of 73.9%, 84.2%, and 88.5% from those of the fin-and-tube heat exchanger.

A 7kW domestic air conditioning system using either a fin-and-tube condenser or a microchannel condenser with the same face area was experimentally examined by Yun et al. in 2006. In comparison to the base system, they discovered that the system with a microchannel heat exchanger had a reduced refrigerant charge amount of 10%, an increased coefficient of performance of 6% to 10%, and an increased SEER of 7%. Additionally, the system's condensing pressure is reduced by 100 kPa, and the pressure drop across the condenser is cut by 84%. The household air conditioning system's SEER is increased by the microchannel heat exchanger because it offers higher heat transfers at smaller pressure reductions.

Air conditioning systems using a microchannel condenser and a round-tube condenser that had nearly comparable frontal area and depth were experimentally compared by Park and Hrnjak (2008). The system with the microchannel condenser showed a notable performance boost. The microchannel condenser system had a 13.1% higher COP than the circular condenser system. Additionally, utilising a microchannel condenser led to a condensing temperature that was 2.5°C lower and a refrigerant pressure drop that was 57 kPa as opposed to 166 kPa in the round-tube condenser. The system with the microchannel condenser had a refrigerant charge that was 9.2% less than the system with the round-tube condenser. The round tube condenser now has a cost advantage despite the fact that the microchannel condenser demonstrated superior heat transfer performance of capacity and system COP.

Wu et al. conducted an experimental investigation of two types of condensers for R22 residential air conditioning systems, one with a round-tube condenser and the other with a microchannel condenser (2009). The experimental findings indicate that a microchannel condenser is a good candidate for a domestic air conditioning condenser since it increases refrigeration power by up to 5% and reduces refrigerant charge by up to 50% with a round tube heat exchanger that has a third of the face area.

In most of the tested and simulated cases, the charge reduction by using the microchannel heat exchanger was up to 21% and the performance were marginally worse. Illan Gomez et al. (2017) compared a minichannel heat exchanger and a conventional fin and tube heat exchanger working as condensers for a residential air-to-water chiller using R134a. Additionally, they discovered that the subcooling is the crucial element in having a powerful charge reduction.

In a heat pump prototype, an MCHX was presented and evaluated by Zanetti et al. (2018). The MCHX's performance was compared to that of a traditional RTPF-HX. When acting as an evaporator, the microchannel heat exchanger exhibits the same heat transfer efficiency as the round tube and plain fin heat exchanger at the same inlet air temperature and velocity. It also ensures greater efficiency when acting as a condenser and lowers the air-side pressure drop. When used as a condenser, the two heat exchangers' internal charges were compared, and it was discovered that the microchannel heat exchanger could reduce this charge by roughly 30%.

According to Aljubury and Mohammed's experimental comparison of conventional air-cooled and microchannel condensers in the automotive vapour compression refrigeration cycle, which uses R134a as a refrigerant, the microchannel condenser has refrigerant side and air side heat transfer coefficients that are, respectively, 224% and 77% higher than those of the conventional condenser. As a result, it was discovered that the COP was 20% greater when utilising the microchannel condenser than it was with the standard cycle. Furthermore, the volume of the microchannel condenser is 50% smaller than that of the ordinary.

CHAPTER 3: MICROCHANNEL CONDENSERS

In a vapour compression cycle, the condenser's job is to receive the hot, high-pressure gas from the compressor and cool it enough that the refrigerant will condense back into a liquid by first removing the superheat and then the latent heat. The liquid is typically also slightly subcooled. The cooling medium will almost always be either air or water.

A refrigerator or freezer, for example, may be able to use its exterior metal covering as a surface condenser due to the limited condensing surface it needs. The condenser tube is held in close mechanical contact with the skin in such a structure, allowing heat to be transferred through to the outside air and lost through natural convection. The maximum power for this system is a few hundred watts.

3.1 HEAT TO BE REMOVED

The heat to be removed in the condenser is shown in the *p–h* diagram (Fig. 3.1).

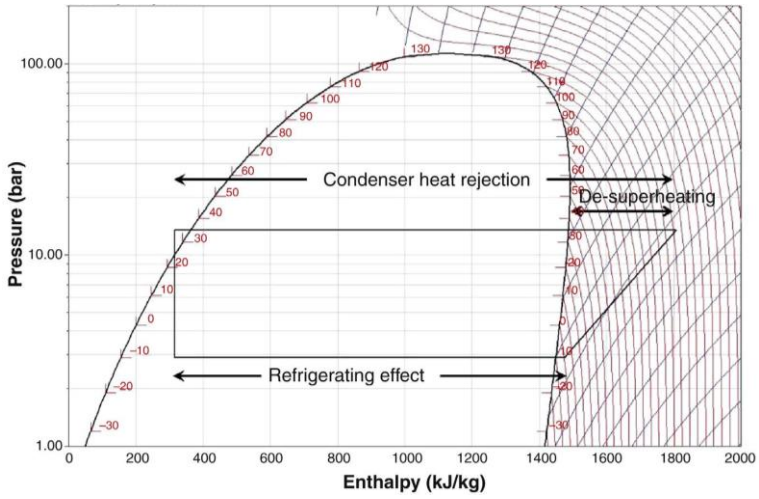

Fig. 3.1 Condenser load *p–h* diagram (Hundy et al., 2016)

Part of this heat is de-superheating. Apart from comparatively small heat losses and gains through the circuit, the total heat rejection will be:

Heat taken in by evaporator + heat of compression.

Again neglecting minute heat gains and losses, the latter will serve as the power input for the compressor, providing:

Evaporator load + compressor input power = condenser load

The rate of heat rejection is referred to as the condenser load. According to the evaporator load and a "de-rating" factor that is based on the evaporating and condensing temperatures, certain manufacturers rate their products.

Evaporator load × factor = condenser load

3.2 AIR-COOLED CONDENSERS

The simplest air-cooled condenser is a simple tube that contains the refrigerant and relies on natural air circulation in still air. The condenser of a household refrigerator is one example; it may also contain some secondary surface in the shape of wires serving as spacers and supports.

Above this size, forced convection, or fans, will be used to move air over the condenser surface. All but the tiniest condensers employ an extended surface due to the high thermal resistance of the boundary layer on the air side of the heat exchanger.

In typical condensers, this takes the shape of copper or aluminium plate fins that are physically attached to copper or aluminium refrigerant tubes. Outside to inner surface ratios typically range from 5:1 to 10:1. Gravity helps the liquid refrigerant flow, therefore the condenser's inlet will be at the top and its outlet at the bottom. Designing pipes that rise should be avoided, and levelling the pipes during installation requires care. Air may move horizontally or vertically upward. Air flows radially inward and out through a fan at the top of small cylindrical matrices.

Because air has a high specific volume and low specific heat capacity, a large volume must be used to dissipate condenser heat. Lower plant efficiency results from an increase in condensing temperature and pressure when the mass flow is decreased.

The condenser must be installed where such a continuous flow of fresh ambient air is available in order for the cooling air to have the coldest feasible temperature. The usage of air-cooled condensers is constrained by the huge air flows required, the power required to move them, and the noise levels that occur.

The temperature difference between the air inlet (ambient) temperature and the condensing temperature will rise as the condenser load rises in order to reject heat more quickly with the same surface area. With a steady airflow, that is. As a first approximation, a condenser rating of kW/K, where K is the temperature differential and kW is the condenser load, can be thought of as constant.

Finned tube condensers can be made of stainless steel, copper, or aluminium for various refrigerants, or aluminium or copper fins on copper or aluminium tube for ammonia.

3.3 MICROCHANNEL CONDENSERS

Coil technology has been concentrating more and more on microchannel technology lately. All- aluminum brazed fin structure is used in microchannel condenser coils. The flat microchannel tube, the fins between the microchannel tubes, and the two refrigerant headers make up the coil as shown in Fig. 3.2 and 3.3. It is constructed of parallel flow aluminium tubes that are mechanically brazed to enhanced aluminium fins, resulting in better heat transfer coefficient and a corrosion resistant, compact and lighter coil

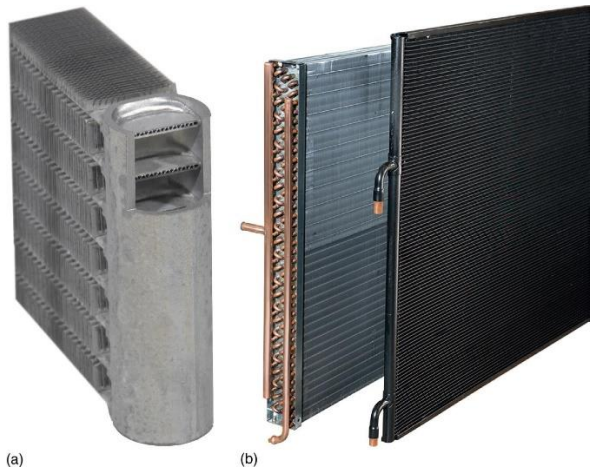

Fig. 3.2 (a) Microchannel condenser cut away view, (b) microchannel condenser (right) alongside conventional finned tube condenser (Hundy et al., 2016)

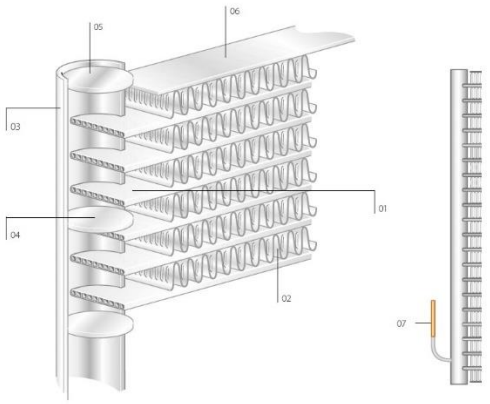

1. Tube
2. Fin
3. Header
4. Baffles
5. End cap
6. Side plate
7. Connections

Fig. 3.3. Parts of a microchannel condenser

The 1980s saw the introduction of this strategy in the automotive sector, and advancements in manufacturing methods have made it possible to manufacture larger units appropriate for industrial systems at a reasonable cost. A brazing furnace with nitrogen gas is used to fuse the parts into a single coil. Since there is only one braze

needed as opposed to 200 or 300 manually brazed connections with conventional copper/aluminum coils, product quality and integrity are maximised. By installing baffles in the distribution headers, it is possible to circuit the refrigerant flow through the flat tubes. The following benefits may be provided by microchannel condensers:

- **Thermal Performance:** The flat tubes, which maximise airside heat transfer, and the microchannels within the tubes, which maximise refrigerant side heat transfer, are what make it substantially superior than a typical Al/Cu coil. Increased main surface area is provided by the small refrigerant tubes. Additionally, the braze operation's metallurgical fin-tube bond maximises surface contact and expands the heat transfer surface area, significantly enhancing heat transfer performance.
- **Corrosion Protection:** As there are no metals that can start galvanic processes, there is less chance of corrosion.
- **Reduced Refrigerant Charge:** Condenser charges that are less than 50% of those of a typical unit can reduce system TEWI values while saving money.
- **Durability:** Construction of microchannel coils reduces weight significantly while improving durability. Leak probabilities are drastically decreased. Two-part epoxy can be used to fix them. Less than 1-inch-thick coils make it simple to remove any trash. A high-pressure sprayer can be used to wash them without damaging the fins.

Cost is the main factor in the sluggish adoption of microchannel. A microchannel unit lends itself to a few tiny, uniform sizes and high-volume production since it is "cast" in a defined block. Because of this, the microchannel has become economically viable in the automotive sector. With various configurations, the commercial refrigeration, air conditioning, and heat pump (RACHP) markets require many fewer units annually. This has a large impact on the volume equation and subsequent cost per unit.

A larger temperature differential than for water-cooled condensers is typically permitted, and condensing temperatures may be 5-8 K higher for a given cooling medium temperature. This is due to the high material cost for air-cooled condensers. When compared to conventional coils, microchannel technology can reduce energy consumption by several degrees.

Microchannel condensers, mostly used in automobile applications and recently in stationary systems, are typically arranged as in Fig. 3.4. Fig. 3.4(a) presents a condenser

without designated subcooling pass and Fig. 3.4 (b) presents a design with integrated receiver-drier which provides designated subcooling.

Multi-pass design provides opportunity for the search of maximized performance by changing mass flux as condensate is formed, affecting local heat transfer on refrigerant side and pressure drop.

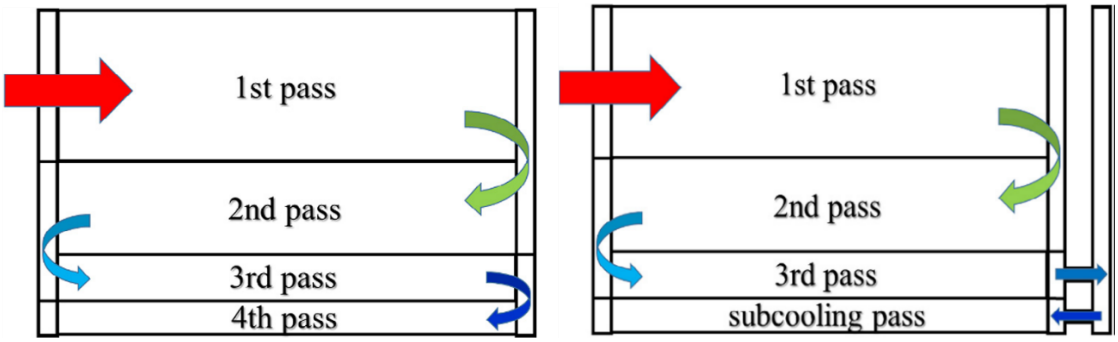

(a) Without designated subcooler (b) With designated subcooler

Fig. 3.4 Traditional condensers (Li and Hrnjak, 2017a)

3.4 CONVECTION IN SMALL DIAMETER CHANNELS

Eqn. 3.1 shows Newton's law of cooling, which governs convective heat transfer from a surface.

$$Q = hA(T_b - T_w) \tag{3.1}$$

Generally, the temperature limits are be fixed. As a result, by increasing the product hA, the heat transfer rate can be increased. Since microchannels have their dimensions in the range of 10 µm - 1000 µm, etching deep and narrow microchannels at the backside of a silicon substrate would increase the surface area for heat transfer. For a fully developed internal flow, the Nusselt number Nu is constant as given by:

$$Nu = \frac{hD}{k} \tag{3.2}$$

Rearranging for h

$$h = Nu\frac{k}{D} \tag{3.3}$$

h is inversely proportional to the microchannel diameter, at a constant Nusselt number. The microchannels possess the advantage of very high h value because of their smaller diameter values. Hence for microchannels, a considerable hA value results in more significant convective heat transfer. This makes microchannel a suitable candidate among various high heat removal options of the order of 100 W/cm² or more.

Typically, the number of tubes in the circuit is reduced, providing situation as in Fig. 3.5. After a short single-phase zone for superheated vapour from compressor discharge, the heat transfer coefficient (HTC) on refrigerant side soon elevates to maximum when the vapour quality equals to 1. Then, HTC has a general falling trend and the kink at the beginning of each pass is due to mass flux increase.

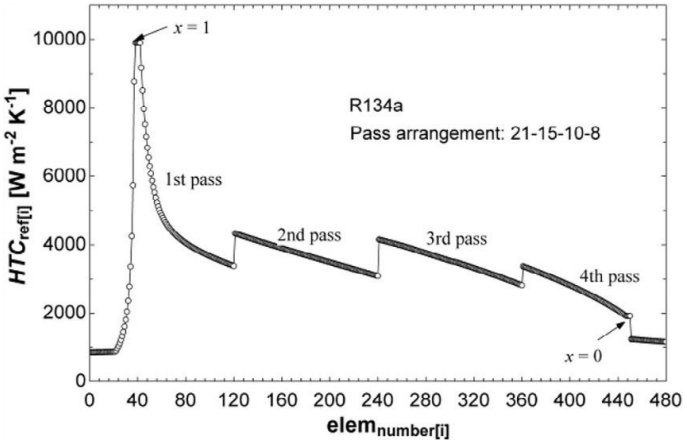

Fig. 3.5 Local heat transfer coefficient on the refrigerant side in a traditional condenser (Li and Hrnjak, 2017)

CHAPTER 4: COMPUTATIONAL FLUID DYNAMICS

4.1 INTRODUCTION TO CFD

Computational Fluid Dynamics (CFD) is one of the branches of fluid mechanics that uses numerical methods and algorithms to solve and analyze problems that involve fluid flows. Computers are used to perform the millions of calculations required to simulate the interaction of fluids and gases with the complex surfaces used in engineering. CFD predicts what will happen, quantitatively, when fluid flow, often with the complications of

- Simultaneous flow of heat
- Mass transfer
- Phase change
- Chemical reaction
- Mechanical movement
- Stress and displacement of immersed solids

4.2 APPLICATIONS OF CFD

- Aerodynamics of aircrafts and vehicles; lift and drag
- Hydrodynamics of ships
- Power plants; combustion in IC engines and gas turbines
- Turbo machinery; flow inside rotating passages
- Metrology; weather predictions
- External and internal environment of buildings; wind loading

4.3 NUMERICAL METHODS IN CFD

The methods used in CFD are

(i) Finite Difference Method (FDM)

(ii) Finite Element Method (FEM)

(iii) Finite Volume Method (FVM)

4.3.1 Finite Difference Method (FDM)

The simplest numerical technique to apply for the solution of the heat/diffusion equation is the finite difference method. The basic idea behind the method is to replace the various derivatives appearing in the mathematical formulation of the problem by suitable approximations on finite difference mesh of nodes. The simplest derivation of finite difference formulae makes use of Taylor series. The final set of linear algebraic equations is solved by any numerical techniques.

4.3.2 Finite Element Method (FEM)

The finite element method sub divides the calculation domain into element, such as triangular rectangles, tetrahedral or rectangular parallelepipeds elements. These elements are considered to inter connected at specified joints called nodes. Here the variation of field variable is inside a finite element can be approximated by a simple function. These approximating functions are defined in terms of the values of the field variables at the nodes. When field equations are written for whole continuum the new unknowns are at the nodal points. By solving the field equations, which are generally in the form of matrix equations, the node values of the field's variables will be known. Once these are known, approximating functions define the field variable through the assemblage of elements.

4.3.3 Finite Volume Method (FVM)

This is the classical or standard approach used most often in commercial software and research coded. An alternative discretization method is based on the idea of regarding the computation domain as subdivided into a collection of finite volumes. In this view, each finite volume is represented by a line in 1D, an area in 2D and volume in 3D. Nodes, located inside each finite volume, become the locus of computational values. In rectangular Cartesian coordinates in 2D the simplest finite volumes are rectangles. For each node, the rectangle faces are formed by drawing perpendiculars through the midpoints between contiguous nodes. Discretization equations are obtained by integrating the original partial differential equation over the span of each finite volume. This method is easily extended to nonlinear problems. The solutions of the algebraic equations are obtained by iterative methods.

One advantage of this method over FDM is that it does not require a structured mesh - although a structured mesh can be used. The FVM can solve problems on irregular

geometries. Furthermore, one advantage of this method over FEM is that it can conserve the variables on a coarse mesh easily. This is an important characteristic of the fluid problem.

4.4 ADVANTAGES OF CFD OVER EXPERIMENT METHODS

CFD analysis results in a substantial reduction of lead time and cost of new design. It is possible to study systems where controlled experiments are difficult or impossible to perform (e.g. very large systems) and also study systems under hazardous conditions. It provides practically unlimited level of detailed results.

The variable cost of an experiment, in terms of facility hire or man-hour costs, is proportional to the number of data points and the number of configurations tested. In contrast CFD codes can produce extremely large volumes of results at virtually no added expense and it is very cheap to perform parametric studies, for instance to optimize equipment performance.

4.5 WORKING OF A CFD CODE

CFD codes are structured around the numerical algorithms that can tackle fluid flow problems. In order to provide easy access to the solving power all commercial CFD packages (Phoenics, Flow3D, Star CD) include sophisticated user interfaces to input problem parameters and to examine the results. All codes contain 3 main elements.

- Pre-Processor
- Solver
- Post-Processor

Pre-processor

Pre-processing consists of the input of a flow problem to a CFD program by means of an operator friendly interface and the subsequent transformation of this input into a form suitable for use by the solver. The user activities at the pre-processing stage involve,

- Definition of the geometry of the region of interests: the computational domain
- Grid generation: the sub-division of the domain into a number of smaller, non-overlapping sub-domains known as grid of cells or mesh (control volumes or elements).
- Selection of the physical and chemical phenomena that need to be modelled.

- Definition of fluid properties.
- Specification of appropriate boundary conditions at cells which coincide with or touch the domain boundary.

The solution to a flow problem is defined at the nodes inside each cell. The accuracy of a CFD solution is governed by the number of cells in each grid.

Solver

There are three distinct streams of numerical solution techniques: finite difference, finite element and spectral methods. In outline the numerical methods that form the basis of the solver perform the following steps.

- Approximation of the unknown flow variables by means of simple functions.
- Discretization by substitution of the approximations into the governing flow equations and subsequent mathematical manipulations.
- Solution of the algebraic equations.

The main differences between the three separate streams are associated with the way in which the flow variables are approximated and with the discretization processes.

Post-processor

As in pre-processing a huge amount of development work has been recently taken place in the post-processing field. The increased popularity of engineering work stations, many of which have outstanding graphics capabilities, the leading CFD packages are now equipped with versatile data visualization tools. These include,

- Domain geometry and grid display
- Vector plots
- Line and shaded contour plots
- 2D and 3D surface plots
- Particle tracking
- View manipulation (translation, rotation, scaling etc.)
- Colour postscript output.

4.6 PROBLEM SOLVING WITH CFD

In solving fluid flow problems, we need to be aware that the underlying physics is complex and the results generated by a CFD code are at best as good as the physics and chemistry embedded in it and at worst as its operator. Prior to setting up and running a CFD simulation there is a stage of identification and formulation of the flow problem in terms of the physical and chemical phenomena that need to be considered. Over 50% of time spent in industry on a CFD project is devoted to the definition of the domain geometry and grid generation.

4.7 COMPUTATIONAL FLUID DYNAMICS SIMULATION

The design, scale-up, and running of unit operations in chemical process industries rely heavily upon empiricism and correlations of overall parameters for non-ideal or non-equilibrium conditions. Many equipment designs in use are based on the experience of experts applying rules of thumb, resembling art more than science. Processes that are sensitive to local phenomena and reactant concentrations are often difficult to design or scale up, because the design correlations do not take local effects into account. Non-idealities introduced by scaling up of lab or pilot scale equipment are difficult, if not impossible to predict accurately.

Researchers, equipment designers, and process engineers are increasingly using computational fluid dynamics (CFD) to analyze the flow and performance of process equipment, such as chemical reactors, stirred tanks, fluidized beds, cyclones, combustion systems, spray dryers, pipeline arrays, heat exchangers and other equipment. CFD allows for in depth analysis of the fluid mechanics, local effects, and chemistry in these types of equipment such as turbulence and combustion. CFD can be used when design correlations or experimental data are not available. It provides comprehensive data that are not easily obtainable from experimental tests. It highlights the root cause, not just the effect and many ‘what if’ scenarios can often be analyzed in a short time. This method reduces scale-up problems, because the models are based on the fundamental physics and are scale-independent.

CFD is basically the science of predicting fluid flow, heat transfer, mass transfer, chemical reactions, and related phenomena by solving the mathematical equations that govern these processes using numerical algorithm. It is the merger of the classical branches of theoretical and experimental science, with the infusion of the modern element

of numerical computation. The results of CFD analyses are relevant engineering data used in conceptual studies of new designs, detailed product development, troubleshooting, and redesign. In many cases, CFD results in better insight, improved performance, better reliability, more confident scale-up, improved product consistency, and higher plant productivity.

The progress of CFD during the last fifty years has been extraordinary. Much of this progress has been driven by the phenomenal increases in digital computing speed. The continual and exponential increase in computing power, improved physical models in many CFD codes, and better user interfaces now enables non-experts to use CFD as a design tool on day-to-day basis. As a consequence, CFD has progressed from the domain of mainframe to the high-end engineering workstation and even to laptop PCs. This power of digital computing has transformed research and engineering especially in fluid mechanics, just as it has in virtually all fields of human endeavours.

4.8 PHASES OF MODELLING AND SIMULATION

There has been a long history of efforts to establish the basic concepts and terminology in modelling and computer simulation. The identification of the fundamental issues and debates began two decades ago in the operation research community, long before there was such concern in the CFD community. The term model, modelling, and simulation are used in a wide range of disciplines. Consequently, these terms have a range of meanings that are both context-specific and discipline-specific. Model is a representation of a physical system or process intended to enhance our ability to understand, predict, or control its behaviour. Modelling is the process of construction or modification of a model. Simulation is the exercise or use of a model.

The basic phases of modelling and simulation have been identified by operation research community. Fig. 4.1 shows these basic phases and processes. It identifies two types of models: a conceptual model and a computer model. The conceptual model is composed of all the information, mathematical modelling data, and mathematical equations that describe the physical system or process of interest. The conceptual model is produced by analysis and observations of the physical system. In CFD, the conceptual model is dominated by partial differential equations. The computer model is an operational computer program that implements a conceptual model. Modern terminology refers to the computer model as computer code.

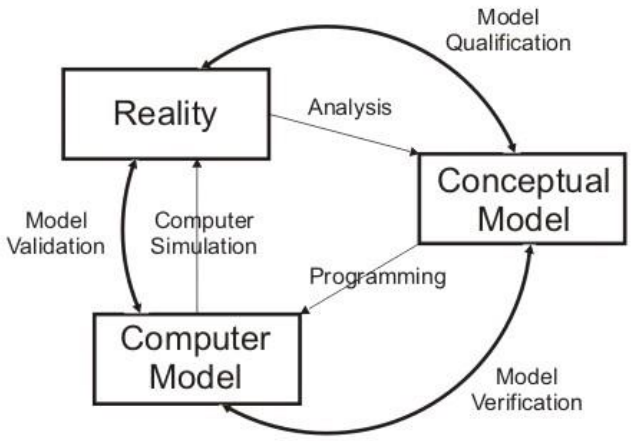

Fig. 4.1 Phases of modelling and simulation

Although CFD simulations are widely conducted in industry, government and academia, there is presently little agreement on procedures for assessing their capability. There is no fixed level of credibility or accuracy that is applicable to all CFD simulations. The accuracy level required of simulations depends on the purposes for which the simulations are intended to be used.

The two main principles that are necessary for assessing credibility are verification and validation. Verification is the process of determining if a computational simulation accurately represents the conceptual description of the model and the solution to the model, but no claim is made of the relationship of the simulation to real world. Validation is the process of determining if a computational simulation accurately represents the real world from the perspective of the intended uses of the model. The definition of verification and validation also stress the evaluation of accuracy. In verification activities, accuracy is generally measured with the respect to benchmark solutions of simplified model problems. In validation activities, accuracy is measured with respect to experimental data, which represent the reality.

Uncertainty and error can be considered as the broad categories that are normally associated with the loss in accuracy in modelling and simulation. Uncertainty is defined as a potential deficiency in any phase or activity of the modelling process that is due to lack of knowledge. Lack of knowledge is commonly caused by incomplete knowledge of a physical characteristic or parameter. Lack of knowledge can also be caused by the complexity of a physical process, for example in the case turbulent combustion. Error is defined as a recognizable deficiency in any phase or activity of modelling and simulation

that is not due to the lack of knowledge. Error can be categorized as either acknowledged or unacknowledged. Examples of acknowledged errors are round- off error in a digital computer and physical approximations made to simplify the modelling of a physical process. Unacknowledged errors include blunders and mistakes such as programming errors.

In CFD simulations, there are four predominant sources of error, namely insufficient spatial discretization convergence, insufficient temporal discretization convergence, lack of iterative convergence, and computer programming. The most important activity in verification testing is to systematically refining the grid size and the time step. The objective of this activity is to estimate the discretization error of numerical solution. As the grid size and time step approach zero, the discretization error should asymptotically approach zero. In verification activities, comparing a computational solution to a highly accurate solution is the most accurate and reliable way to quantitatively measure the error in the computational solution. However highly accurate solutions are known for a relatively small number of simplified problems. These highly accurate solutions can be classified into three types: analytical solutions, benchmark numerical solutions to ordinary differential, and benchmark numerical solutions to partial differential equations.

4.9 CFD CALCULATION

CFD is applied by first dividing or discretizing the geometry of interest into a number of computational cells. Discretization is the method of approximating the differential equations by a system of algebraic equations for the variables at some set of discrete locations in space and time. The discrete locations are referred to as the grid or the mesh.

The continuous information from the exact solution of the Navier-Stokes partial differential equations is now replaced with discrete values. The number of cells can vary from a few thousands for a simple problem to millions for very large and complicated ones. Cells have a variety of shapes. Triangular and quadrilateral cells are generally used in 2D problems. For 3D problems, hexahedral, tetrahedral, pyramidal, and prismatic shaped cells can be used.

In the past, CFD codes required the use of structured grids containing one cell type, such as brick-shaped hexahedral elements, in which the cells were positioned in regular pattern. Current codes allow cells to be located in an irregular, unstructured pattern, giving much greater geometric flexibility. Additionally, a good CFD code can accept

grids consisting of a combination of different cell types, or hybrid grids, to address complex geometries, providing flexibility to the CFD analyst. Geometries are often created using computer aided design (CAD) software. The geometry, either a wire frame or solid model is exported to the grid-generation software program to create the CFD quality grid. A few packages have combined both functions of CAD geometry creation and mesh generation into a single interface. With the grid created, the boundary conditions such as pressures, velocities, mass flows, and scalars specified, and physical properties defined, the CFD calculations can start. The CFD codes will solve the appropriate conservation equations for all grid cells using iterative procedure. Typical chemical process applications involve solving for: mass conservation (using a continuity equation), momentum (using Navier Stokes equations), enthalpy, turbulent kinetic energy, turbulent energy dissipation rate, chemical species concentrations, local reaction rates, and local volume fractions for multiphase problems.

There are many commercial CFD packages for modelling and analyzing system involving fluid flow, heat transfer and associated phenomena such as chemical reaction. Some popular CFD packages include: FLUENT, CFX, PHOENICS and ANSYS. All these commercial CFD codes contain three main elements: Pre- processor, Solver and Post-processor. This study concentrates on the use of ANSYS 19.2 software package to simulate the flow and mixing behaviour especially for chemical and thermal industrial applications.

4.10 ANSYS 19.2 ANALYSIS

CFD analysis has been carried to study the heat transfer in a jet impingement system. Once the important features of the problem are determined, the following procedural steps are of be followed.

- Define modelling goals.
- Create the model geometry and grid.
- Set up solver and physical models.
- Compute and monitor solution.
- Examine and save results.
- Consider revision to numerical or physical model parameters.

1. Defining modelling goals.

2. Creating model geometry and grid

Ansys 19.2 is used for reducing time spend for generating mesh and simplifying geometry modelling. Ansys 19.2 is capable of handling triangular and quadrilateral elements in 2D and hexahedral & pyramid in 3D

3. Setting up the solved and physical models, for a given problem, we need to,

- Import and check the grids.
- Select the numerical solver.
- Select appropriate physical models.
- Define material properties.
- Prescribe operating conditions and boundary conditions.
- Proved initial solutions.
- Initialized flow fields.

4. Computing and monitoring the solutions.

- The discretized conservation equations are solved relatively.
- Convergence is reached when,

  a) Change in solution variables from one iteration to next are negligible.

  b) Residuals provide mechanism to help monitor this trend.

  c) Overall property conservation is achieved.
- The accuracy of converged solutions depends upon,

  a) Approximation and accuracy of models

  b) Grid resolutions

  c) Problem set up

5. Examining and saving results,

- Visualization tools can be used to see flow patterns and key flow features can be resolved.

- Numerical reporting tools can be used to calculate average heat transfer coefficient, flex balances etc.

6. Revising the model

Once the solution is converged the following questions are considered for analyzing the solutions.

- Are physical models appropriate?
- Are boundary conditions, correct?
- Is grid adequate?

CHAPTER 5: NUMERICAL ANALYSIS

The first step in CFD analysis is to create a geometric model of the issue domain. The geometric model is created, and then it is meshed to discretize it. Specifying the input data, defining the material qualities, and defining the boundary conditions are done after meshing. The solution setup is then initialized, and computations are carried out for the designated amount of time. After the calculations are finished, post processing is carried out to extract the data pertaining to the key variables.

5.1 SIMULATION OF FLUID FLOW THROUGH MICROCHANNEL

ANSYS Fluent 19.2, is used in simulating heat transfer between hot fluid and the cold channel inner surfaces in various inlet areas and the results are compared with findings of Xia and Chan (2015). Pressure drop is also studied.

5.1.1 Geometrical Model and Meshing of Microchannel

In order to simulate the heat transfer taking place in it, micro channel model is generated using Design Modeler in ANSYS Fluent. Fig. 5.1(a) shows the model geometry set up while Fig. 5.1(b) shows the grids which possess cuboid shape with the same volume. As shown in Fig. 5.1(a), inlet and outlet are the two terminating surfaces in Z direction. Other four surfaces which are perpendicular to the inlet are the walls of the channel. Therefore, the walls perpendicular to the Y axis are the top and bottom walls, and the ones perpendicular to the X axis are left and right walls, respectively.

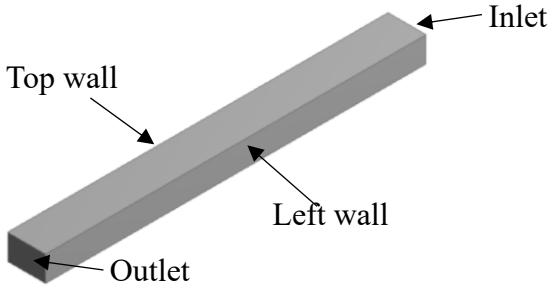

Fig. 5.1(a) Geometry set-up of the channel

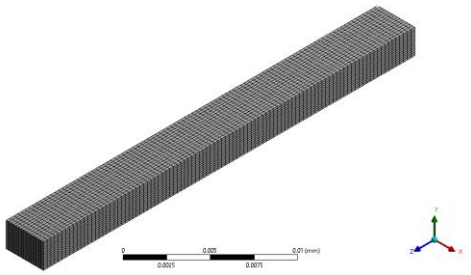

Fig. 5.1(b) Meshing of the microchannel

A grid independence study is conducted with number of elements ranging from 10000 to 184900 and grid size with 122500 elements is selected. The results of grid independence study are shown in the Fig. 5.2. It can be found that further refinement of mesh could not make any notable progress in the accuracy of the result.

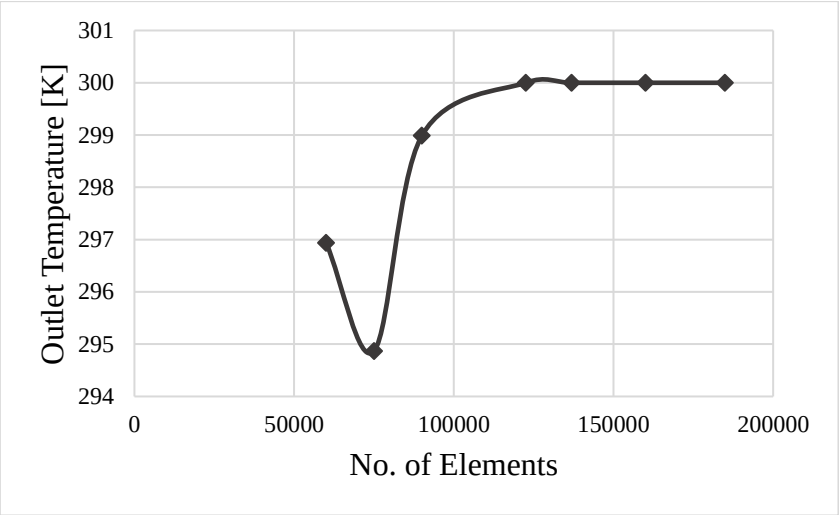

Fig. 5.2 Grid independence test for the microchannel geometry

To investigate the size effect of micro channel on heat transfer, the cross-sectional area of the channel is varied. Table 5.1 shows the variation of length (in X direction as shown in Fig. 5.1) and width (in Y direction as shown in Fig. 5.1), the variation of area, and the ratio of heat transfer area to volume of channel. It can be seen that the ratio of heat transfer area to volume decreases as the inlet area increases.

Table 5.1 Variation of the cross-sectional area of micro channel

No.	Length	Width	Area	Ratio of heat transfer area to volume
	μm	μm	μm^2	μm^{-1}
1	3	2	6	0.5
2	6	4	24	0.25
3	12	8	96	0.125
4	18	12	213	0.0833
5	24	16	384	0.0625
6	30	20	600	0.05

5.1.2 Boundary Conditions and Calculation Models Used in Simulation

Hot air flows from the inlet towards the outlet and exchanges its heat with the cold top and bottom walls. Boundary conditions which are shown in Table 5.2 are applied in the simulation. In this simulation, the continuity, momentum and energy conservation equations are solved. Also, Standard k-ε model is used to modeling the momentum transport.

Table 5.2 Boundary Conditions

Boundary	Conditions
Inlet	T:400K, v:0.001 m/s
Outlet	Outflow
Top and bottom walls	Non slippery walls and surface temperature: 300 K
Right and left walls	Non-slippery and adiabatic walls

5.2 FLUID FLOW THROUGH MICROCHANNEL HEAT EXCHANGER

This section mainly focuses on modelling a miniaturized cross flow heat exchanger as per Meral and Parlak (2021) and numerical investigation of the heat and fluid flow inside aluminum heat exchanger plate which has square channels under constant wall temperature boundary condition. R22 is also tested with the heat exchanger model.

5.2.1 Geometry and Meshing

The heat exchanger was composed of two thermal exchanger plates in cross flow arrangement. The micro heat exchangers studied in this work has an architecture based on a large number of parallel microchannels showing a square cross section connected to two common manifolds. The microchannel plates that make up the heat exchanger were made of aluminum and these plates are 3mm thick. It has 31 microchannels on both plates where hot and cold-water passes. All microchannels were 30 mm long. 31 each microchannel is designed and manufactured with width and height equal to 490 umm. Geometrical dimensions of the tested micro heat exchanger are shown in Table 5.3.

Table 5.3 Dimensions of the micro heat exchanger

Geometrical details	Value
Number of channels	31
Channels width	490 μm
Channel height	490 μm
Channel length	30 mm
Dimensions of the plate	50×50×50 mm
Thickness of the plate	3 mm

Fluid flow path for the micro-channel plate given in Fig. 5.3 has been modelled with SOLIDWORKS drawing program and defined in order to be analyzed in FLUENT.

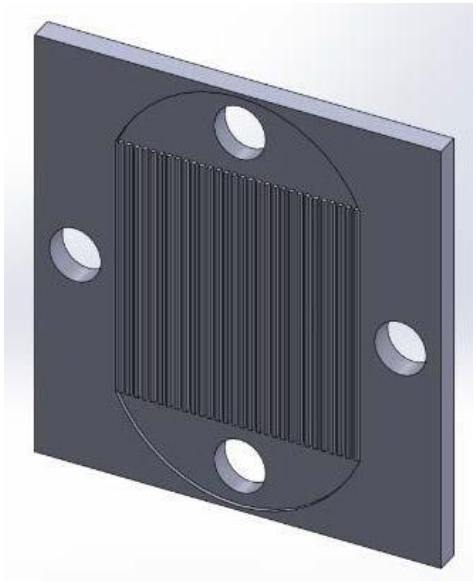

Fig. 5.3 3D drawing of the microchannel plate (Meral and Parlak, 2021)

The meshing has been done and grid independence test was also conducted for the mesh. Grid size with 2151816 elements is selected. The results of grid independence study are shown in the Fig. 5.4.

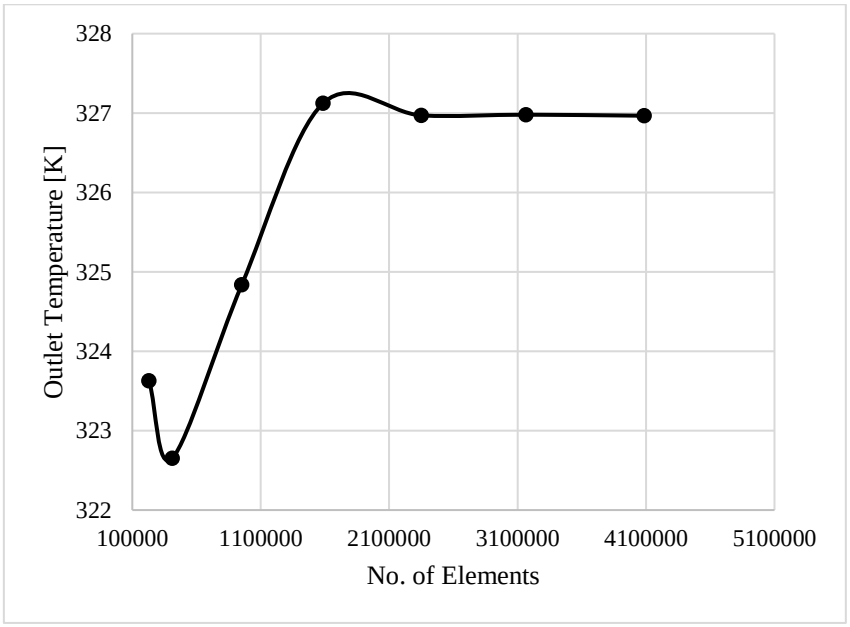

Fig. 5.4 Grid independence test for microchannel heat exchanger geometry

5.2.2 Computational Domain and Boundary Conditions

The fluid flow is assumed incompressible, laminar and viscous dissipation is negligible. Due to the phase change, the upper wall of the plate was assumed to be at constant temperature. At the water outlet uniform atmospheric pressure is applied. The analysis has been conducted for different 20 mass flows rate mentioned under the same conditions.

The image of flow volume of working flow analyzed in ANSYS and all boundaries of the computational domain are marked schematically in Fig. 5.5.

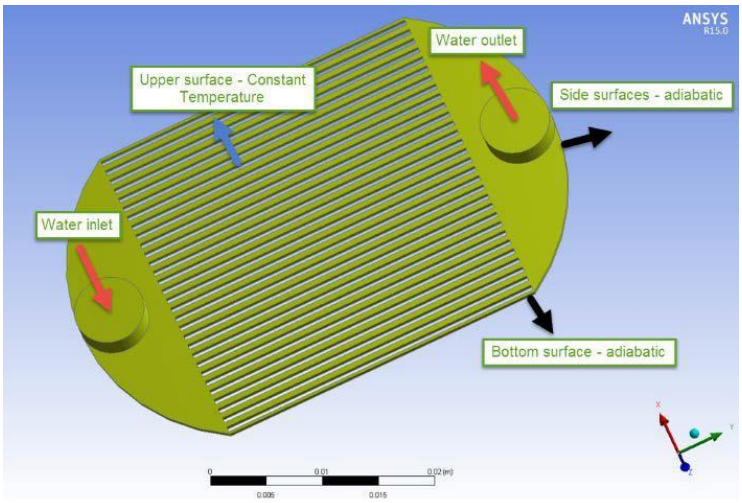

Fig. 5.5 Computational domain and boundary conditions (Meral and Parlak, 2021)

5.3 SIMULATION OF FIN AND TUBE CONDENSER

5.3.1 Geometry

Geometry of fin and tube condenser is modelled with Solidworks. Dimensions of the condenser are given in Table 5.4

Table 5.4 Dimensions of the fin and tube condenser

Geometrical details	Value
Number of rows	2×24
Length of each row	750 mm
Diameter of tube	6.37 mm
Dimensions of the fin	500 ×40× 1 mm

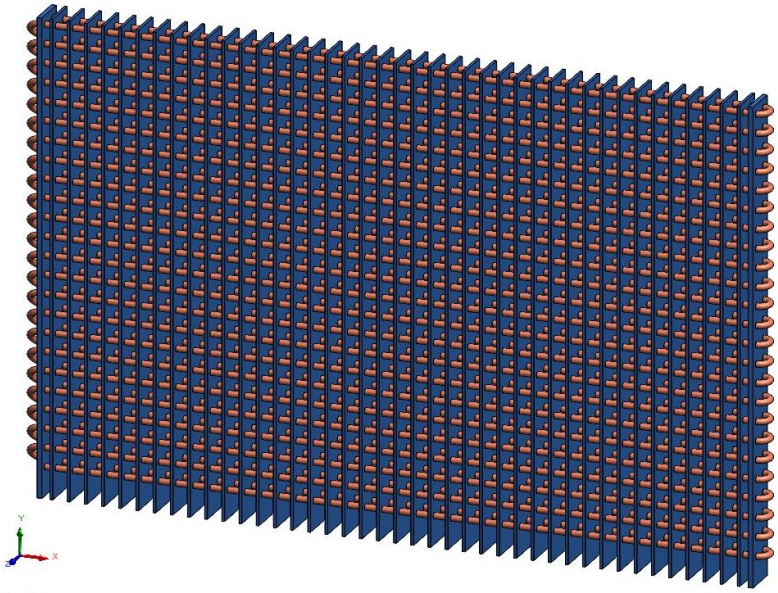

Fig. 5.6 Geometry of fin and tube condenser

Since the whole length of the condenser cannot be processed as a single file in ANSYS FLUENT, length of condenser is reduced to one fourth of the original length as shown in Fig. 5.7. for further analysis.

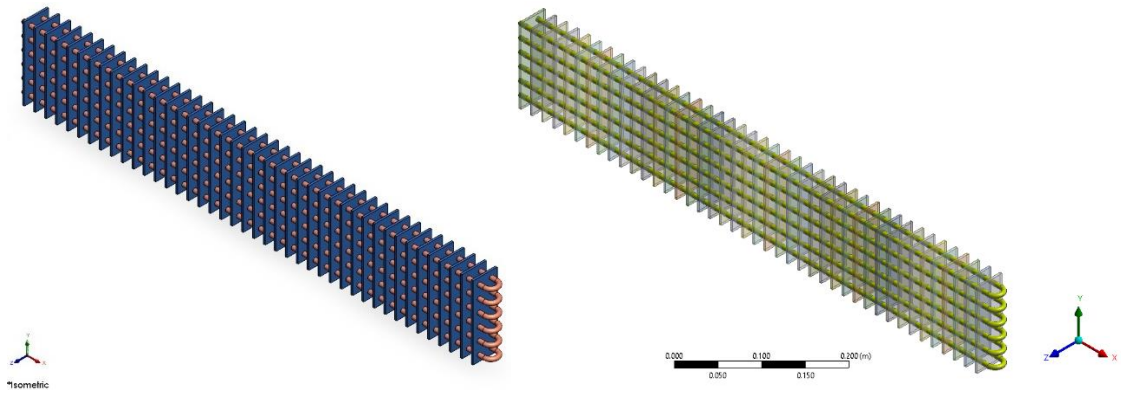

Fig. 5.7 Geometry of part of fin and tube condenser for analysis

5.3.2 Meshing

After the geometric model has been developed, the following stage in CFD analysis is to build the meshing of the computational area. During mesh creation, the problem domain is divided into a large number of tiny cells. To mimic physical events, the CFD application solves multiple equations for each cell. The results of the simulation are significantly influenced by the number of cells in the domain. To imitate the physical occurrences, the domain must have a sufficient number of cells. As the number of cells rises, so does the amount of time it takes the solver to discover a solution. Therefore, it is always important to determine the ideal number of cells that can run a simulation in a reasonable amount

of time while still producing results that are sufficiently accurate. The best number of cells for a domain typically relies on how challenging the problem is and how much simulation time is available. A high-quality mesh is necessary for a precise CFD analysis. Tetrahedral mesh was chosen for discretization in this work.

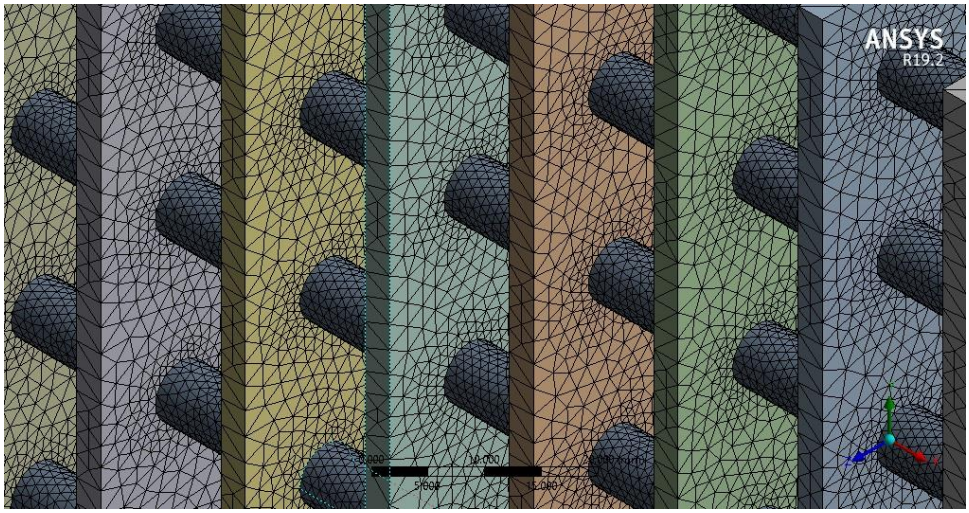

Fig. 5.8 Meshing for the condenser geometry

For various numbers of elements, a grid independence test is conducted, and the inner surface temperature of double glazing is noted. It demonstrates that for 3582486 elements, the temperature difference is minimal.

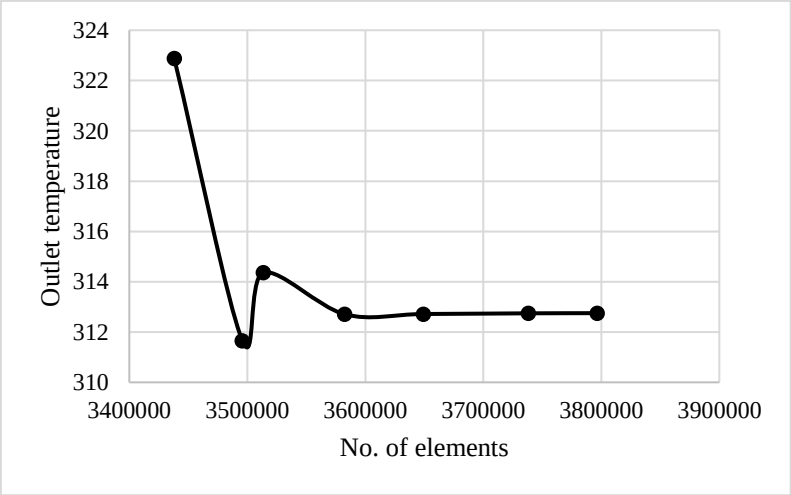

Fig. 5.9 Grid independence test for condenser geometry

Once the mesh has been created, it must be checked for quality. The skewness and aspect ratio of the generated mesh have been studied in this work as two parameters. An element with a skewness value of 0 is considered perfect by the skewness criteria, while elements having a skewness value greater than zero are not regarded as being of high quality. An element with a skewness value of 1 is typically regarded as being unviable. In a well-

meshed domain, there must be a very tiny or negligible number of elements having a skewness value of 1. The average skewness value for a mesh of excellent quality must always be less than 0.3. It is found to be less than 0.001. Another metric used to assess how well a produced mesh is done is aspect ratio, which is comparable to this. An acceptable mesh should have an aspect ratio of no more than two on average.

5.3.3 Boundary Conditions

For an accurate solution to a fluid flow problem, it is crucial to define the appropriate boundary types and boundary conditions. While some boundary conditions are set by simulation software, the majority are defined by physical phenomena. The interfaces are configured to be thermally linked, and the calculated heat transfer coefficient values are given to the refrigerant pipe as well as to the fins. The experimentally determined compressor discharge temperature serves as the condenser model's inlet temperature.

Calculation of heat transfer coefficient for the fins:

The film temperature, $T_f = \frac{40+25}{2} = 30°C$

The physical properties of air at 30°C are:

$\rho = 1.165$ kg/m^3, $c_p = 1005$ J/kgK, $v = 16.00\times10^{-6}$m^2/s, $k = 0.02675$ W/mK, $Pr = 0.701$

$x = 0.1$ m

$$Re_x = \frac{u_\infty x}{v} = \frac{5\times0.1}{16.00\times10^{-6}} = 31250 = 3.1\times10^4$$

$$Nu_x = \frac{h_x x}{k} = 0.332 Re_x^{1/2} Pr^{1/3}$$

$$= (0.332)(31250)^{1/2}(0.701)^{1/3}$$

$$= 52.14$$

$$h_x = \frac{Nu_x k}{x} = \frac{52.14\times(0.02675)}{0.1} = 13.94 \text{ W/mK}$$

The average value of the heat transfer coefficient is twice this value or,

$$\bar{h_x} = (2)(13.94) = 27.88 \text{W/mK}$$

Calculation of heat transfer coefficient for the refrigerant tube:

The film temperature, $T_f = \frac{95+25}{2} = 60°C$

The physical properties of air at 60°C are:

$\rho = 1.060$ kg/m^3, c_p=1005 J/kgK, $v = 18.97\times10^{-6}$m^2/s, $k = 0.02896$ W/mK, $Pr = 0.696$

$$Re_D = \frac{uD}{v} = \frac{5\times(6.36\times10^{-3})}{18.97\times10^{-6}} = 1676.33$$

$$Re_D Pr = 1676.33 \times 0.696 = 1166.7 > 0.2$$

Equation given by Sachdeva (2012) can be used to calculate the average Nusselt number

$$\overline{Nu_D} = 0.3 + \frac{0.62 Re_x^{1/2} Pr^{1/3}}{[1+(0.4/Pr)^{2/3}]^{1/4}}\left[1+\left(\frac{Re_D}{28200}\right)^{5/8}\right]^{4/5} \quad \text{(Sachdeva,2012)}$$

$$\overline{Nu_D} = 0.3 + \frac{0.62(1676.33)^{1/2}(0.696)^{1/3}}{[1+(0.4/0.696)^{2/3}]^{1/4}}\left[1+\left(\frac{1676.33}{28200}\right)^{5/8}\right]^{4/5}$$

$$\overline{Nu_D} = 22.68$$

And the heat transfer coefficient,

$$\bar{h} = \frac{\overline{Nu_D} k}{D} = \frac{(22.68)(0.02896)}{(6.36\times10^{-3})} = 103.272 \text{ W/mK}$$

5.3.3.1 Input Parameters

Certain parameter values, such as material qualities and beginning parameter values must be entered as input parameters into the CFD tool. The table contains the values for the input parameters.

Table 5.5 Input parameters

Function	**Specification**	
Solver	Energy	On
	Type	Pressure-based
	Time	Steady
	Viscous model	Standard k-ε, Standard wall function
Materials	Solid	Copper
	Fluid	R22 ($CHClF_2$)

5.3.3.2 Solution Technique

A discretization strategy is needed to solve the governing equations and scalar variables like temperature. For this work, two discretization schemes are pertinent: -

- First Order Upwind, in which the values of the cell faces are specified to be equal to those of the cell centres in cells upstream, and
- Second Order Upwind, where the Taylor Series expansion is used to determine the cell face values in order to enhance the range of the surrounding cells' influences.

A stable solution is provided by the First Order upwind solution method, which also exhibits a good rate of residual convergence. This plan's drawback is that the solution's accuracy could not be adequate. Therefore, where great precision is not the primary objective, the first order upwind technique can be employed. The Second Order upwind approach, on the other hand, delivers extremely precise simulation results. However, the amount of time needed for the simulation increases significantly when the second order upwind solution technique is used. Therefore, first order upwind solution method was used in the current study by taking into account for the calculation capability and the time available.

5.3.3.3 Convergence Criteria

The solution's convergence is determined by the difference in required parameter i.e., output temperature value after each iteration. Convergence criteria are established under the presumption that the solution would remain unchanged after convergence. One approach to the problem is the pressure-velocity coupling, which employs the SIMPLE system. The parameters were set in Fluent, and then the solution was initialised. Depending on how easily the convergence occurred and how long it took to obtain the results, iterations were performed.

5.4 SIMULATION OF MICROCHANNEL CONDENSER

Refrigerant flow through the microchannel condenser is also modelled in ANSYS Fluent. Microchannel condenser having the same face area of the fin and tube condenser is selected. The external dimensions of the microchannel condenser is same as that of the fin and tube condenser.

5.4.1 Geometry

Geometry of microchannel, modelled with Solidworks is shown in Fig. 5.10 and 5.11.

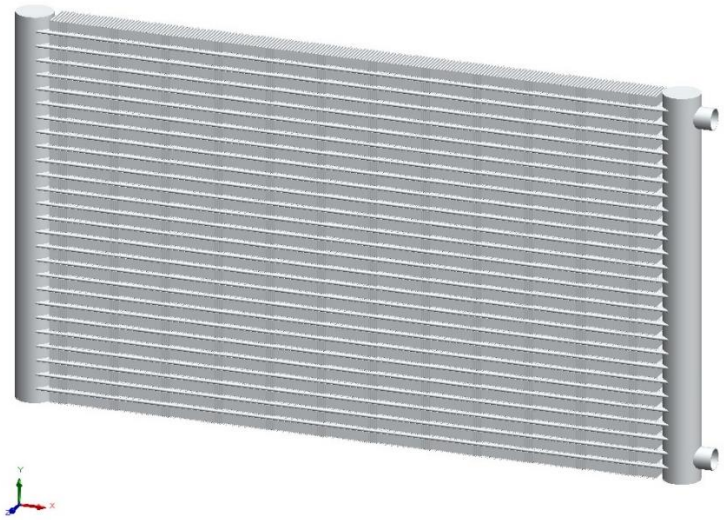

Fig. 5.10 Geometry of microchannel condenser

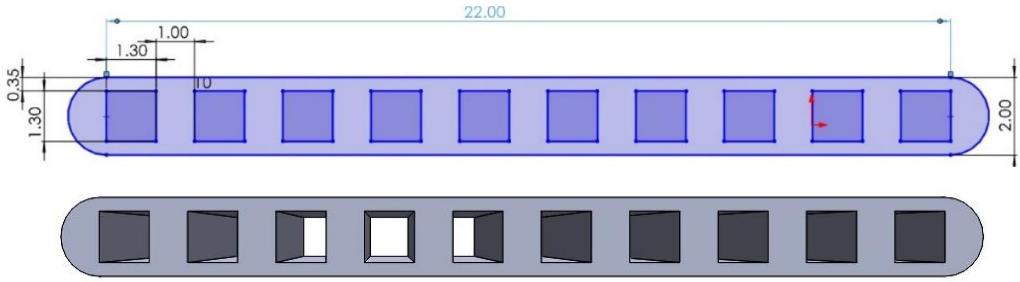

Fig. 5.11 Tubes in the microchannel condenser

Dimensions of the condenser are given in Table 5.6

Table 5.6 Dimensions of the microchannel condenser

Geometrical details	Value
Number of tubes	50
Length of each row	750 mm
Width of tube	22 mm
Height of the fin	8 mm

Since the microchannel condenser has a complex geometry with huge number of components, a single channel is considered for heat transfer analysis.

5.4.2 Meshing

The model was meshed with patch conforming algorithm with tetrahedrons method. The element was set to default initially and varied for the grid independency test.

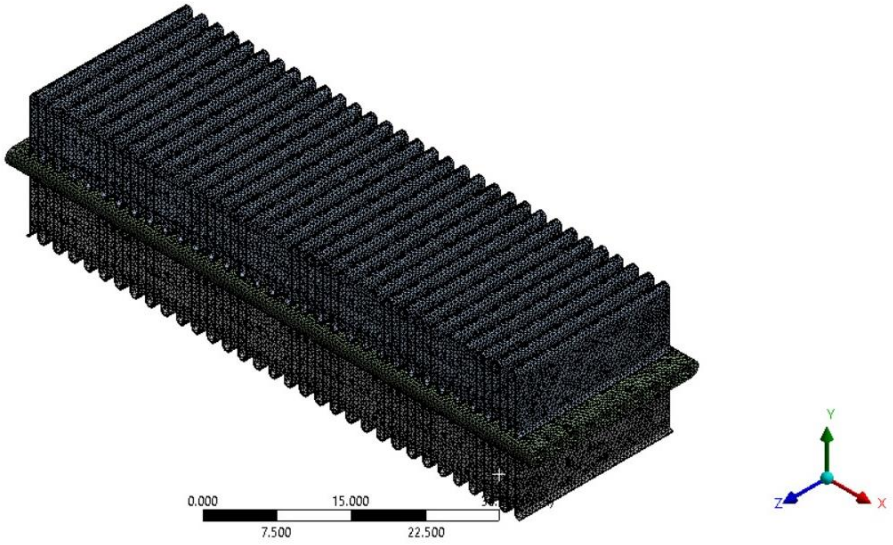

Fig. 5.12 Meshing for the microchannel condenser geometry

After the grid independence test, mesh with 653229 is selected. If the number of elements is increased further, the variation in outlet temperature is negligible.

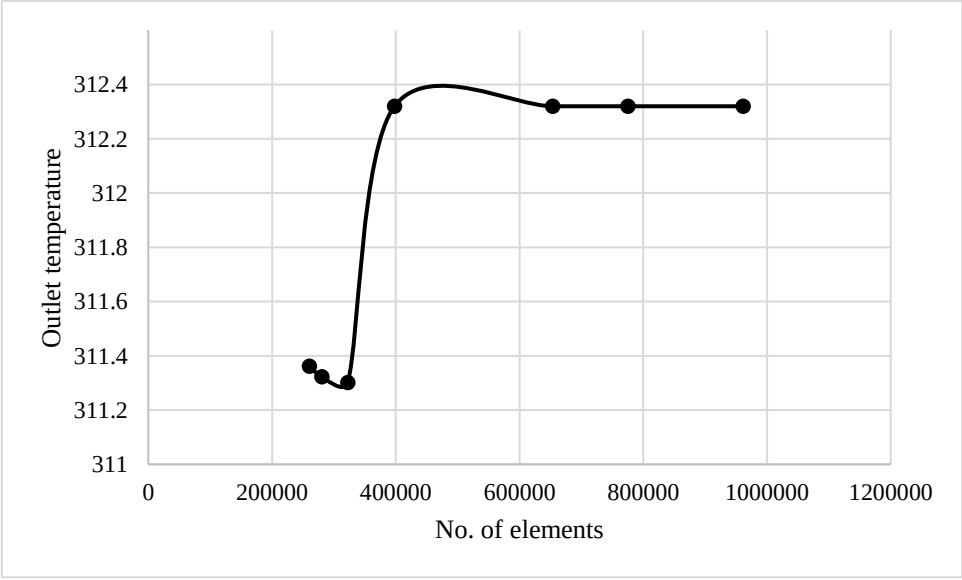

Fig. 5.13 Grid independency test for the microchannel geometry

5.4.3 Boundary Conditions

Flow of water as well as R22 is to be tested with the microchannel condenser. The calculated heat transfer coefficient values are given to the condenser.

Calculation of heat transfer coefficient for the fins:

The film temperature, $T_f = \frac{60+30}{2} = 45°C$

The physical properties of air at 45°C are:

$\rho = 1.110$ kg/m^3, $c_p = 1005$ J/kgK, $v = 17.455\times10^{-6}$ m^2/s, $k = 0.02791$ W/mK, $Pr = 0.6985$

$D = L = 1.3$ mm $= 1.3\times10^{-3}$

$$Re_D = \frac{uD}{v} = \frac{5\times(1.3\times10^{-3})}{17.455\times10^{-6}} = 372.38$$

$Re_D Pr = 372.38 \times 0.6985 = 372.38 > 0.2$

Equation given by Sachdeva (2012) can be used to calculate the average Nusselt number

$$\overline{Nu_D} = 0.3 + \frac{0.62 Re_x^{1/2} Pr^{1/3}}{[1+(0.4/Pr)^{2/3}]^{1/4}}\left[1+\left(\frac{Re_D}{28200}\right)^{5/8}\right]^{4/5} \quad \text{(Sachdeva,2012)}$$

$$\overline{Nu_D} = 0.3 + \frac{0.62(372.38)^{1/2}(0.6985)^{1/3}}{[1+(0.4/0.6985)^{2/3}]^{1/4}}\left[1+\left(\frac{372.38}{28200}\right)^{5/8}\right]^{4/5}$$

$\overline{Nu_D} = 10.106$

And the heat transfer coefficient,

$$\bar{h} = \frac{\overline{Nu_D}k}{D} = \frac{(10.106)(0.02791)}{(1.3\times10^{-3})} = 216.97 \text{ W/mK}$$

All other boundary conditions are maintained constant for the performance comparison between the two condensers.

CHAPTER 6: EXPERIMENTAL ANALYSIS

To enhance the heat transfer of air-cooled condenser in the air conditioning systems, microchannel condenser is employed. The goal of the experiment is to determine the difference in coefficient of performance of the air conditioning system while using the two condensers i.e., copper fin and tube condenser and aluminium microchannel condenser.

6.1 INSTRUMENTATION

The instruments and devices used for the experiment are discussed below.

6.1.1 Thermocouples

Type T thermocouples were used to measure the temperature of refrigerant at inlet and outlet of condenser and evaporator. Four type T thermocouples were used. Type T Thermocouple (Copper/Constantan) has excellent repeatability between –200°C to 200°C. The thermocouples are calibrated using constant temperature water bath. Temperature sensor is used to get the temperature readings from the thermocouples.

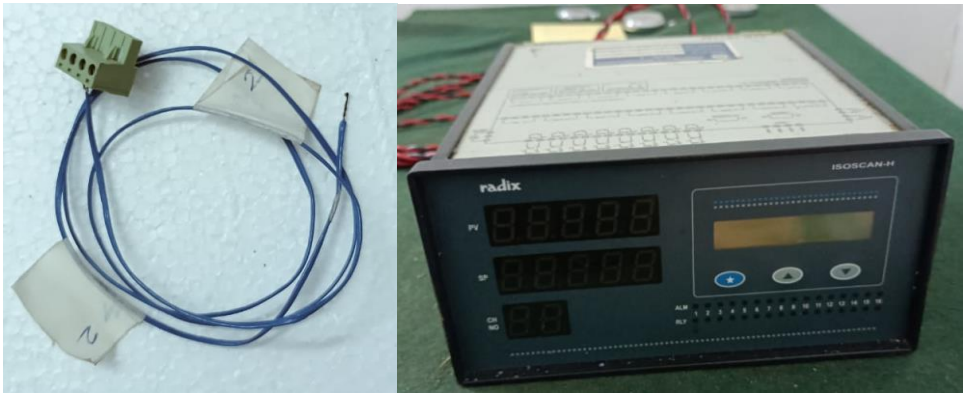

Fig. 6.1 (a) Type T Thermocouple (b) Temperature indicator

6.1.2 Thermometer

Mercury glass thermometer is used.

Range: -10°C to 110°C.

Least count: 1°C.

Fig. 6.2 Mercury-glass thermometer

6.1.3 Pressure Gauge

Analog pressure gauges are used at the low pressure and high-pressure lines.

Range:

LP: -50 bar to 50 bar for R22

HP: -50 bar to 80 bar for R22

Fig. 6.3 Pressure gauges

6.1.4 Hygrometer

Hygrometer which shows temperature as well as humidity measurements are used to measure the temperature and humidity of the tested space.

Fig. 6.4 Hygrometer

6.1.5 Room Heater

Quartz halogen room heater is used for giving heat load to the test space.

Fig. 6.5 Room heater

6.2 CALIBRATION OF THERMOCOUPLE

Fig. 6.5 depicts a schematic representation of the setup for calibrating the thermocouples used in the experiment. For the current experimental work, type T thermocouples are employed. Gas welding is used to create the thermocouple bulbs. The thermocouple bulb is submerged in water that is kept at a constant temperature. A temperature indicator is attached to the thermocouple's opposite end.

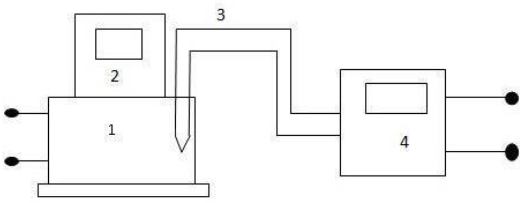

1. Constant temperature bath
2. Temperature display
3. Thermocouple
4. Temperature indicator

Fig. 6.6 Schematic layout of thermocouple calibration

Table 6.1 Calibration data for thermocouple (T1)

Sl. No.	Set Temperature (°C)	Observed Temperature (°C)	Error (%)
1	35	34.4	1.71
2	45	45.5	-1.11
3	50	50.6	-1.20
4	55	55.2	-0.36
5	75	76.7	-2.27
6	95	93.5	1.58

Table 6.2 Calibration data for thermocouple (T2)

Sl. No.	Set Temperature (°C)	Observed Temperature (°C)	Error (%)
1	35	34.5	1.43
2	45	44.2	1.78
3	50	49.4	1.20
4	55	55.4	-0.73
5	75	77.5	-3.33
6	95	96.3	-1.37

Table 6.3 Calibration data for thermocouple (T3)

Sl. No.	Set Temperature (°C)	Observed Temperature (°C)	Error (%)
1	35	34.9	0.29
2	45	44.6	0.89
3	50	49.8	0.40
4	55	54.9	0.18
5	75	74.7	0.40
6	95	95.7	-0.74

Table 6.4 Calibration data for thermocouple (T4)

Sl. No.	Set Temperature (°C)	Observed Temperature (°C)	Error (%)
1	35	34.8	0.57
2	45	44.3	1.56
3	50	49.1	1.80
4	55	54.6	0.73
5	75	74.1	1.20
6	95	94.5	0.53

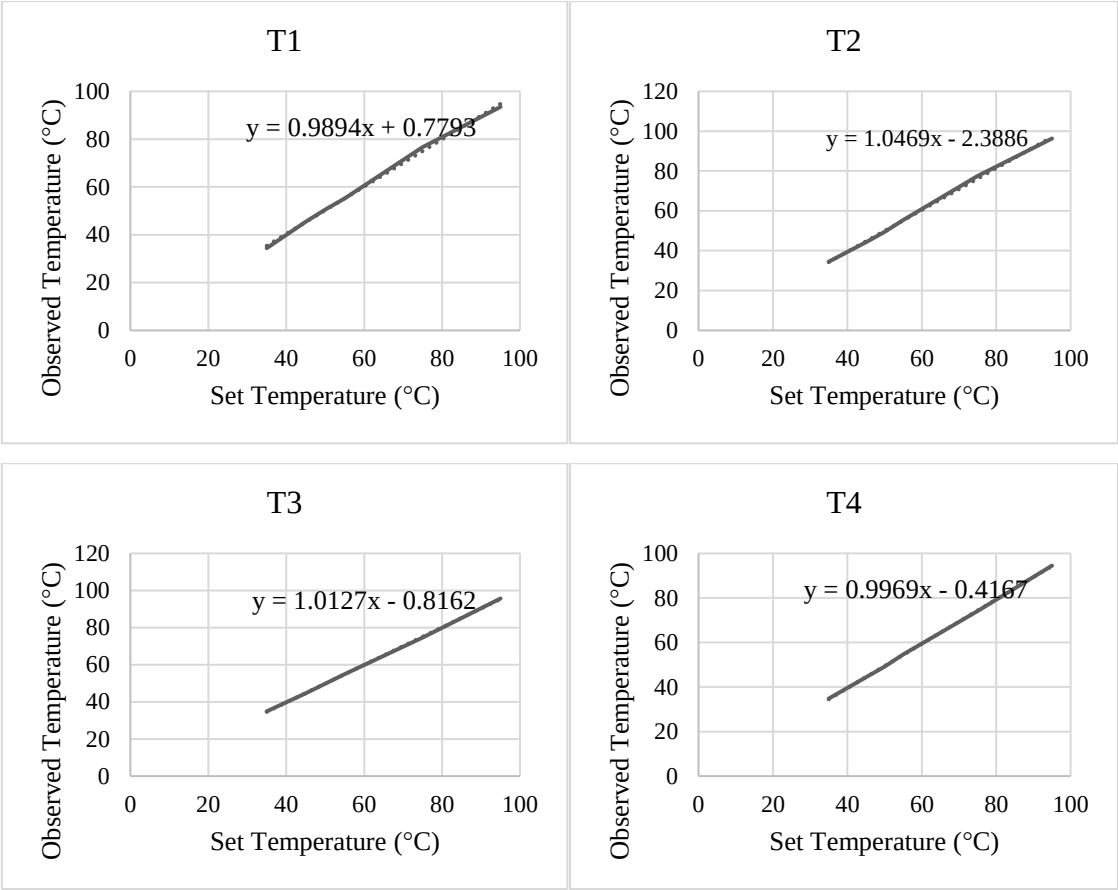

Fig. 6.7 Calibration curve for thermocouples (T1, T2, T3, T4)

6.3 EXPERIMENTAL SETUP

The schematic diagram of the experimental setup is shown in Fig. 6.8.

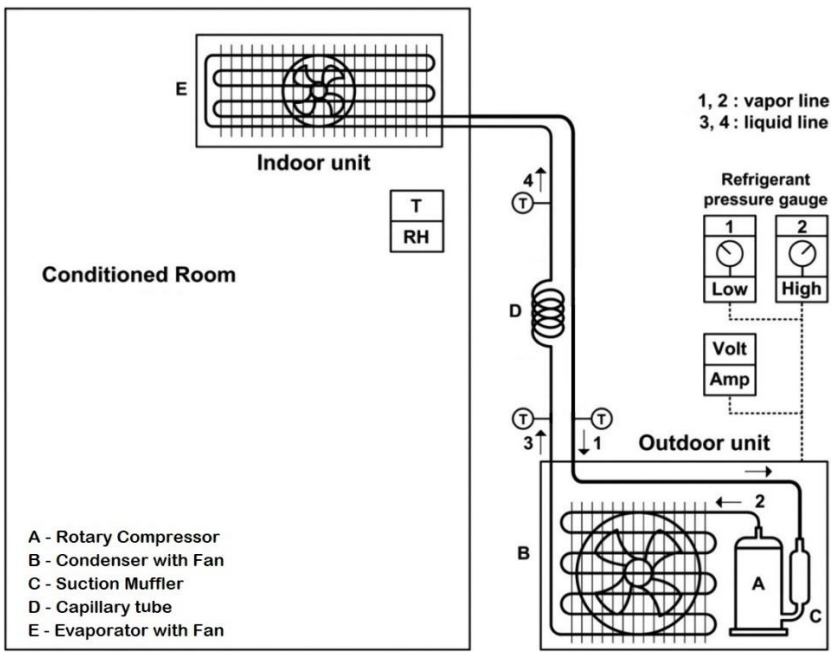

Fig. 6.8 Experimental setup and measurement tools

The test unit used in this study is a residential split air conditioner having a rated cooling capacity of 2TR and R22 as its working fluid. The room air conditioner (RAC) is a split-type under the commercial name of Bluestar and model number HWE-241RB. The specifications of the room air conditioner used in this study are shown in Table 6.5. The indoor and outdoor units are connected with refrigerant pipelines.

Table 6.5 Specification of air conditioner

Item		**Information**	**Unit**
Power Source		1 Phase 220 V 50 Hz	
Cooling Capacity		2	TR
Power Input		2	kW
Current		2	A
Pressure	High	12	bar
	Low	2	bar
Refrigerant		R22	
Refrigerant piping	Liquid line	9.525	mm
	Gas line	15.875	mm

The unit is composed of the basic cycle components, a rotary compressor, a condenser, a capillary tube, and an evaporator as shown in Fig. 6.8. Thermocouples (T1,T2,T3,T4) are connected at the inlet and outlet of evaporator and condenser for temperature measurement. High and low pressure measurements are taken with the pressure gauges. Initial and final DBT and RH are measured with the hygrometer. Multimeter is used to measure the voltage and current for calculation of power consumption of the compressor.

The experiment is done inorder to analyse the improvement in coefficient of performance when the condenser of the air conditioning system is replaced with a microchannel heat exchanger. Initially, the system is run with the normal fin and tube condenser and then the micochannel condenser is installed in the systyem. Temperature as well as pressure readings are taken in both the cases and calculation of COP is done.

Table 6.6 shows the specification of the fin-and-tube and microchannel heat exchangers. They have the same face area and external dimensions. The total number of tubes of the

fin-and-tube heat exchanger is 48, and 50 for the microchannel heat exchanger. The fin-and-tube heat exchanger has a single refrigerant circuit. The microchannel heat exchanger is divided in four parallel tube groups.

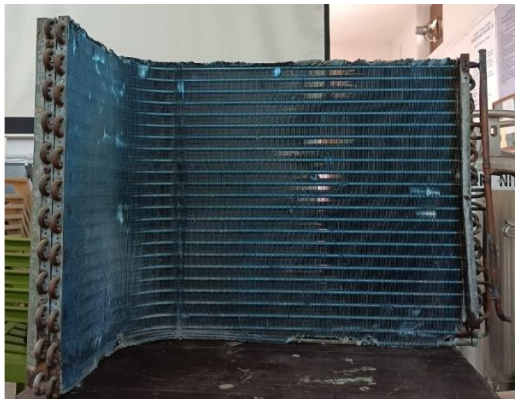

Fig 6.9 Fin and tube condenser

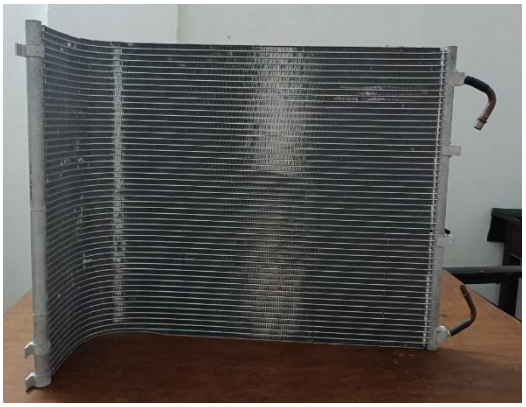

Fig 6.10 Microchannel condenser

Table 6.6 Specifications of test condensers

	Fin and Tube condenser	Microchannel Condenser
Material	Copper	Aluminium
Mass	3.000 kg	4.820 kg
Fin shape	Plate fin	Louvered fin
Number of rows	2	1
Tubes per row	24	50
Dimension	30" × 20"	30" × 20"
Face area	0.375 m^2	0.375 m^2

6.4 PERFORMANCE PARAMETERS

A pressure-enthalpy diagram of the vapour compression refrigeration system is shown in Fig. 6.11.

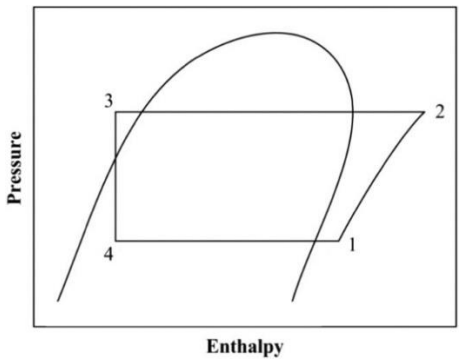

Fig. 6.11 Pressure-enthalpy diagram of the system

The cooling capacity of the RAC system, Q_e(kW), is calculated by the following equation:

$$Q_e = \dot{m}_r(h_6 - h_5) \tag{6.1}$$

where $\dot{m}_r$ is the refrigerant mass flow rate in kg/s obtained by first calculating the power consumption of the experimental setup. In electrical devices such as air conditioners, power can be calculated using the formula:

$$P = V \times I \tag{6.2}$$

where P is the power in kW, V is the voltage in Volts, and I is the current in Amperes. Then the mass flow rate of the refrigerant in the system can be calculated by the equation:

$$\dot{m}_r = \frac{P}{(h_2 - h_1)} \tag{6.3}$$

The COP of an air conditioning system is the ratio of useful cooling provided to the work required. Higher COPs equate to lower operating costs. For complete systems, COP calculations should include energy consumption of all power-consuming auxiliaries. The COP is calculated by the following equation:

$$COP = \frac{Q_e}{P} = \frac{(h_1 - h_4)}{(h_2 - h_1)} \tag{6.4}$$

CHAPTER 7: RESULTS AND DISCUSSION

The results of this study are summarized in three parts: simulation results, experimental results and comparison of the results.

7.1 NUMERICAL ANALYSIS RESULTS

Fluid flow through microchannel, microchannel heat exchanger, normal fin and tube condenser and a microchannel condenser of same dimensions is simulated using ANSYS Fluent.

7.1.1 Fluid Flow Through Microchannel

In this section, simulation results for flow of refrigerant through micro channels with different cross-sectional areas are presented. Fig. 7.1, where the unit of x and y axis is m and K, respectively, shows the distribution of air temperature in terms of middle line for different size channels. It can be found that the air temperature decreases from inlet to outlet in different speeds. The inlet is at 0m and the outlet is at 0.0003m. Temperature drops rapidly when the inlet area is the smallest, i.e., $3\times2\mu m^2$, and it decreases with an increase of the inlet area.

Higher rate in the temperature drop illustrates the stronger heat transfer ability owing to the fact that the heat is dissipated more quickly. Therefore, we find that the heat transfer can be strengthened as the inlet area of the channel is decreased, i.e., the ratio of heat transfer area to volume is increased. This result indicates the size effect on heat transfer varies as the ratio varies. Enhancement of heat transfer can be obtained by increasing the ratio, which has been validated by previous relative researches.

In Fig. 7.2(f), the air temperature drops to 300K at the vicinity of outlet. We can conclude that the air temperature remains higher than 300K if the inlet area is further increased. However, for the smaller sized channel, air temperature decreased to 300K occurring far away from the outlet. The location in channel where air temperature decreases to 300K is different when the inlet area of channel is different.

We could find that micro channel having smaller inlet area has more intensive heat transfer. Therefore, shorter channel with smaller inlet area can be applied to achieve the same amount of heat transfer rate.

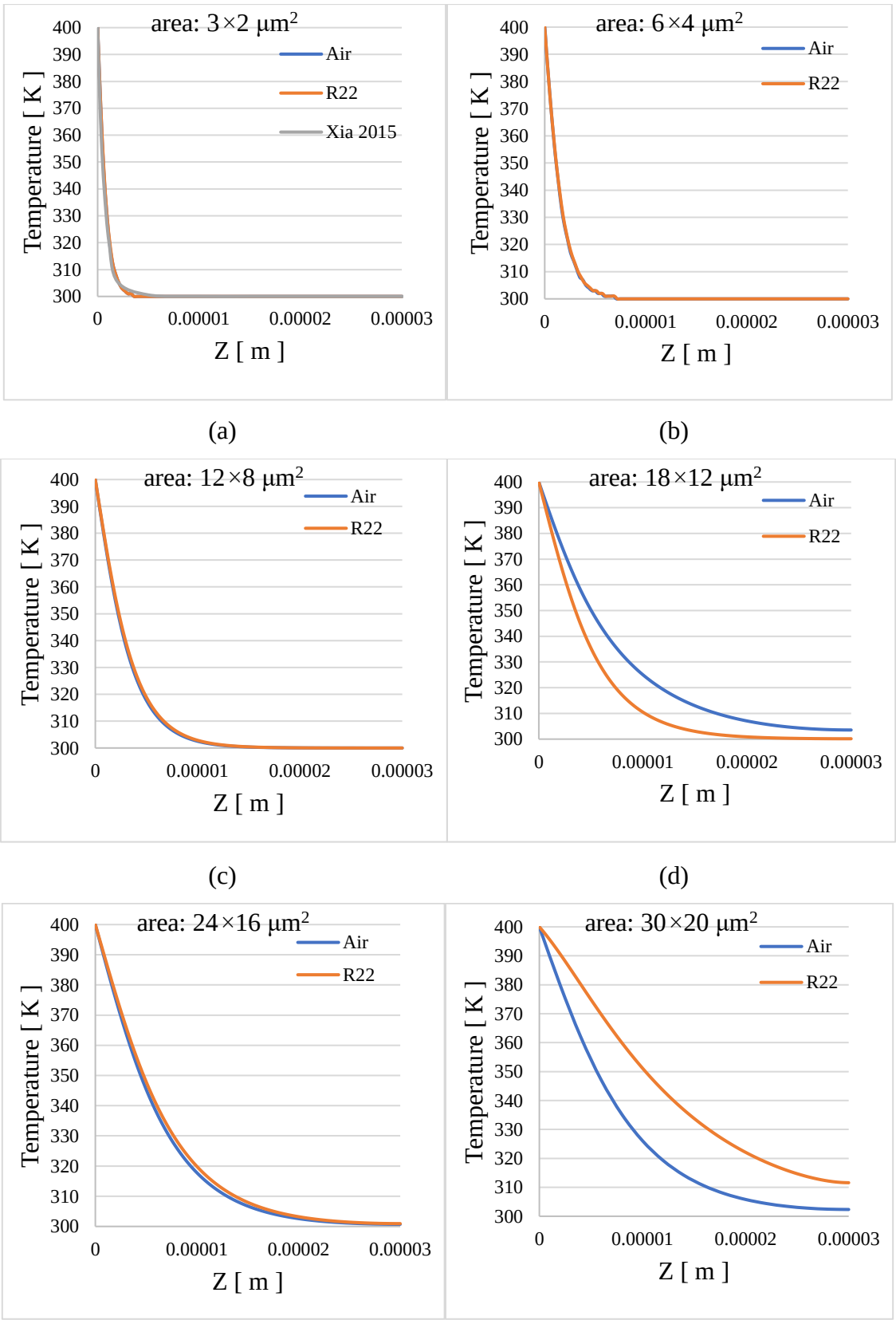

Fig. 7.1 Temperature distribution on the middle line for different inlet areas

Table 7.1 and Fig. 7.2 shows the heat transfer data obtained from the simulation of R22 through the microchannel. And it is evident from the graph that, the channel with smaller inlet area has an upper hand in heat transfer per unit volume of fluid.

Table 7.1 Outlet temperature and heat transfer for R22

No.	Area	Volume	Outlet temperature	Pressure drop	Heat transfer per volume
	μm^2	μm^3	K	Pa	kW/m^3
1	6	180	300	25.38	972.02
2	24	720	300	6.54	685.78
3	96	2880	300.01	1.75	582.81
4	216	6480	300.09	0.84	574.10
5	384	11520	300.59	0.52	536.77
6	600	18000	306.93	0.36	381.13

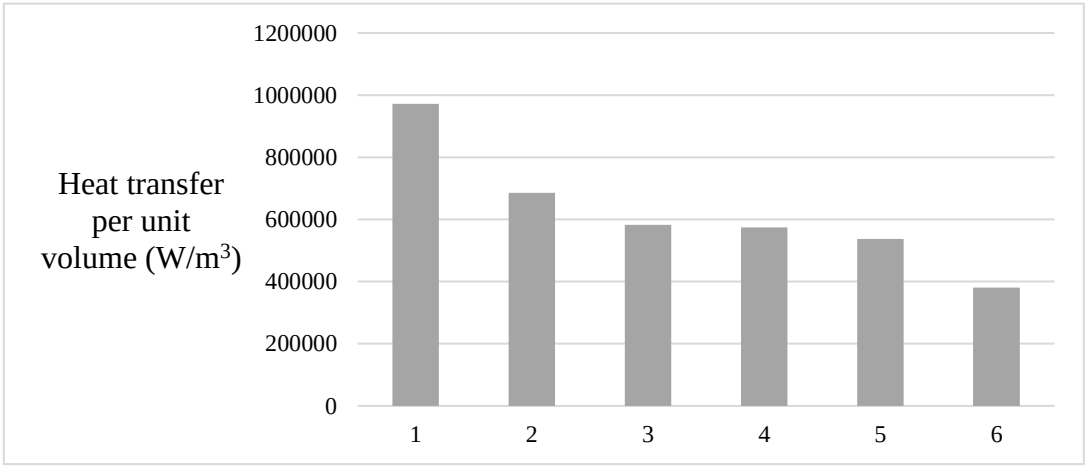

Fig 7.2 Heat transfer per unit volume for each case

7.1.2 Fluid Flow Through Microchannel Heat Exchanger

Air flow through the microchannel geometry from Meral (2021) is done and is compared with the results in the available literature. The pressure and temperature contour for air flow through the heat exchanger is shown in Fig. 7.3. Fig 7.4 shows the variation of outlet temperature with the variation in inlet mass flow rate and the comparison with Meral (2021) is also done.

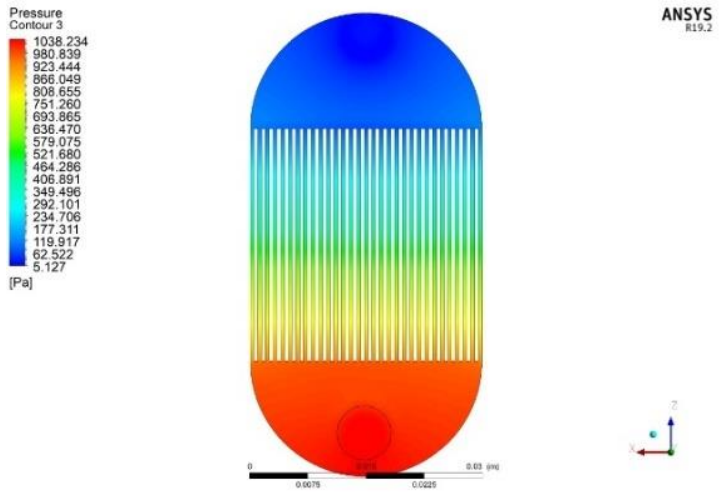

Fig 7.3 (a) Pressure contour for air flow through microchannel heat exchanger

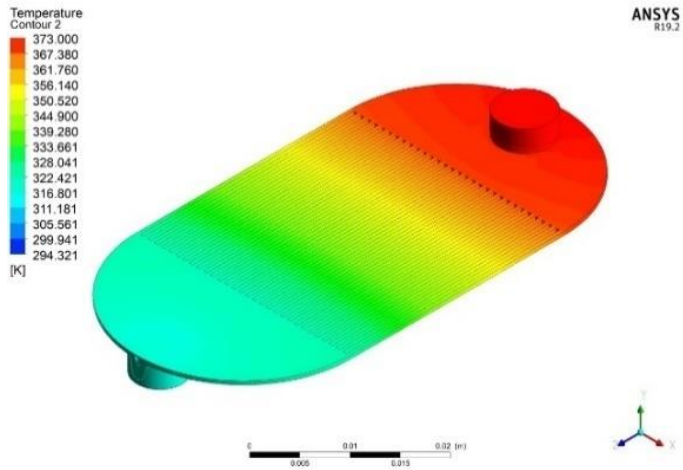

Fig 7.3 (b) Temperature contour for air flow through microchannel heat exchanger

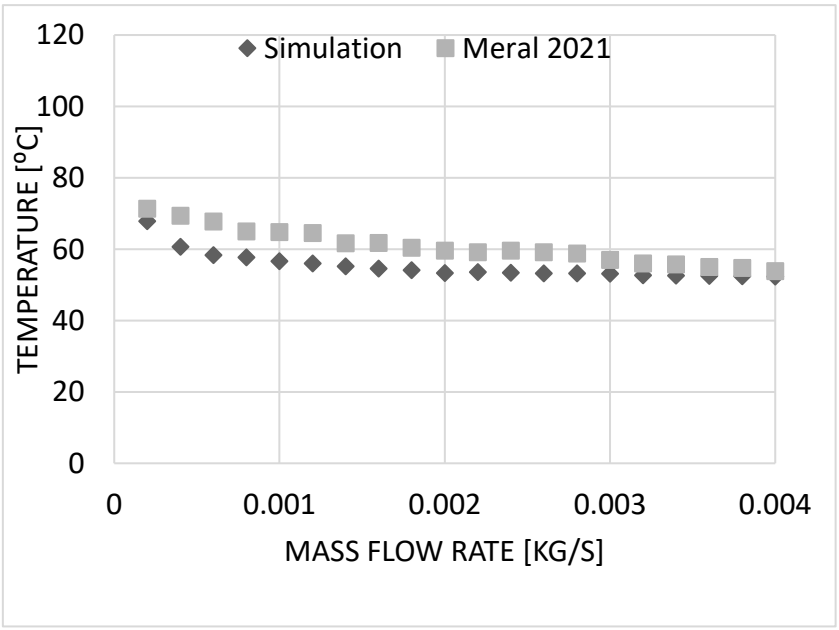

Fig. 7.4 Variation of outlet temperature with mass flow rate

After validation of literature, flow of R22 through the microchannel is simulated and the temperature drop for different mass flow rates are obtained. Temperature contour for flow of R22 through the microchannel heat exchanger is shown in Fig. 7.5.

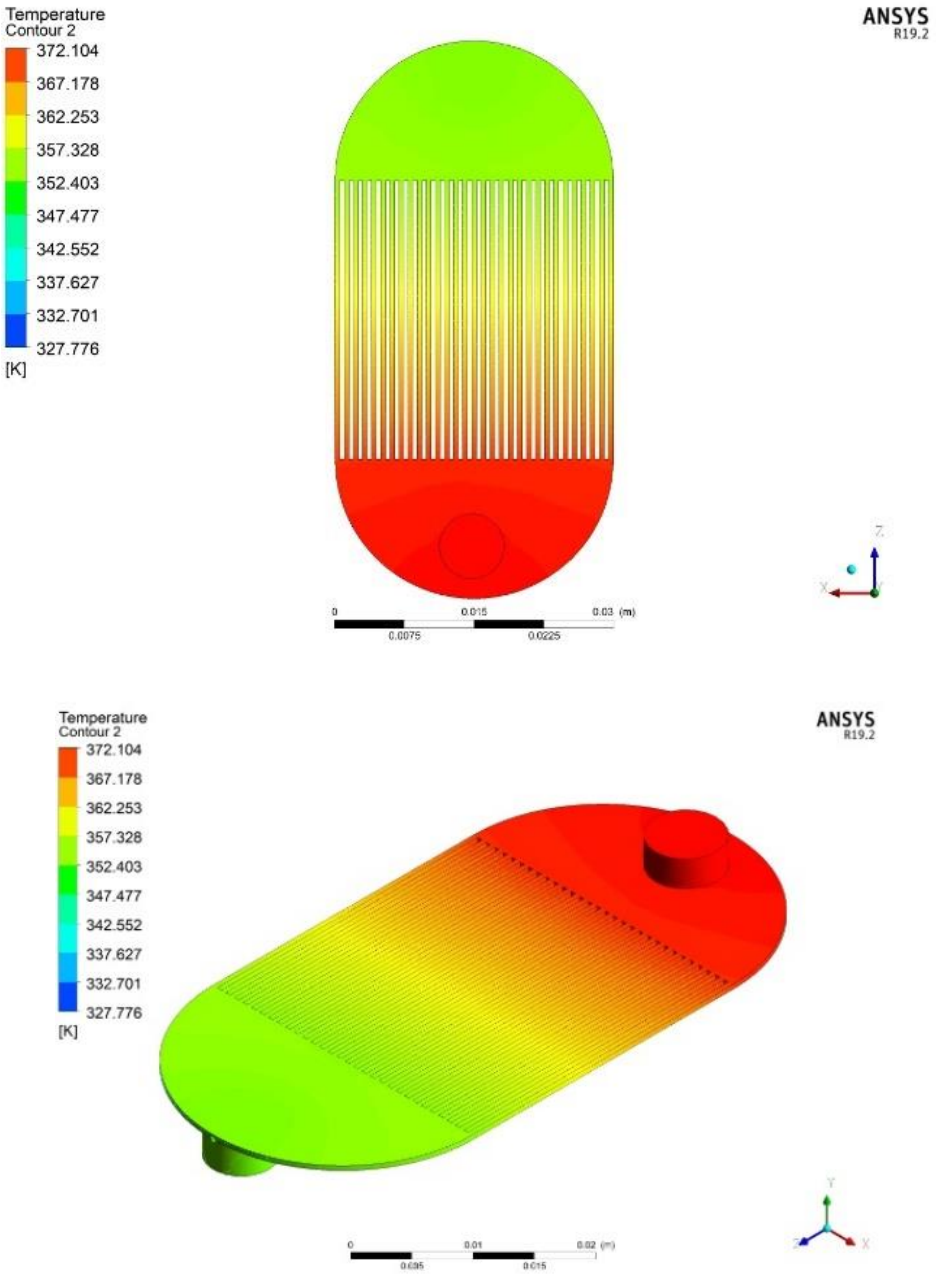

Fig. 7.5 Temperature contour for flow of R22 through microchannel heat exchanger

Variation of outlet temperature with different inlet mass flow rates are plotted in Fig. 7.6. Unlike air, R22 doesn't have much variation in outlet temperature when the inlet mass flow rate is varied.

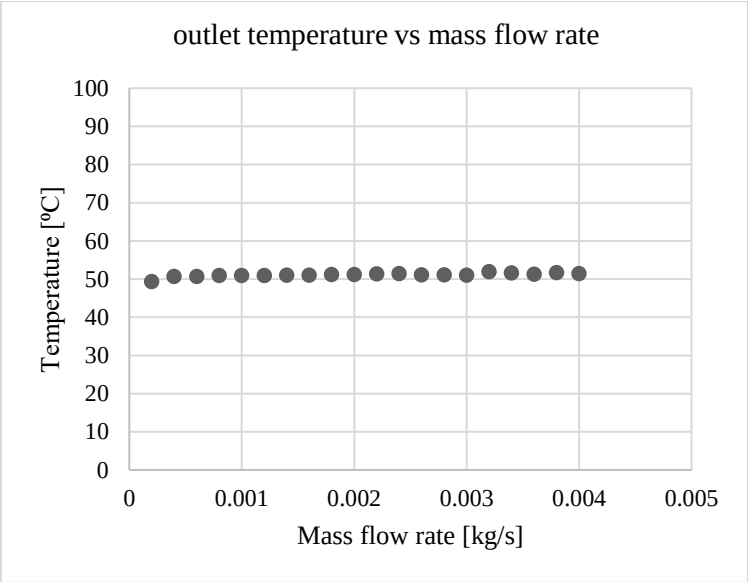

Fig. 7.6 Outlet temperature for R22 in the microchannel heat exchanger

7.1.3 Simulation of Fin and Tube Condenser

Flow of R22 through fin and tube condenser is simulated using the software according to the inlet conditions of the experiment. Temperature and pressure contour are plotted. Outlet temperature is also noted. Calculation of theoretical COP is done from the pressure-enthalpy chart of R22, according to the outlet temperature from the simulation of refrigerant flow through the condenser.

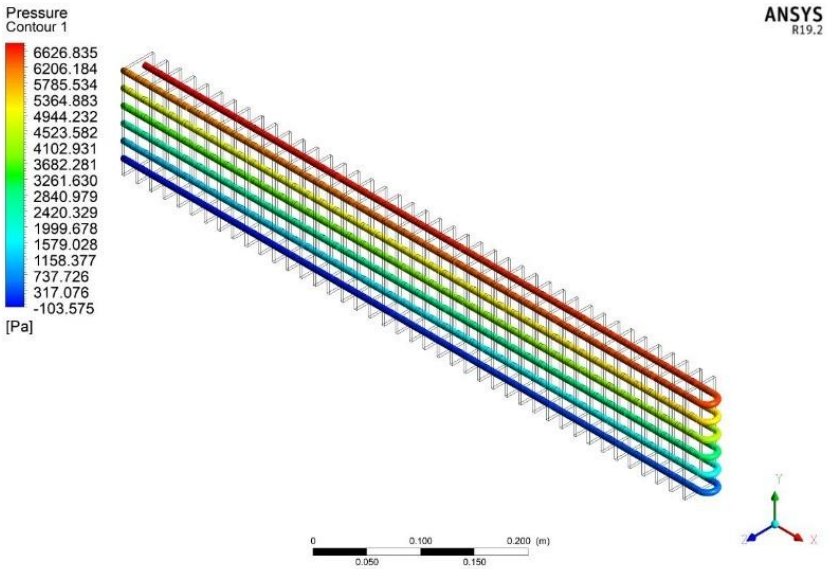

Fig. 7.7 Pressure contour of fin and tube condenser

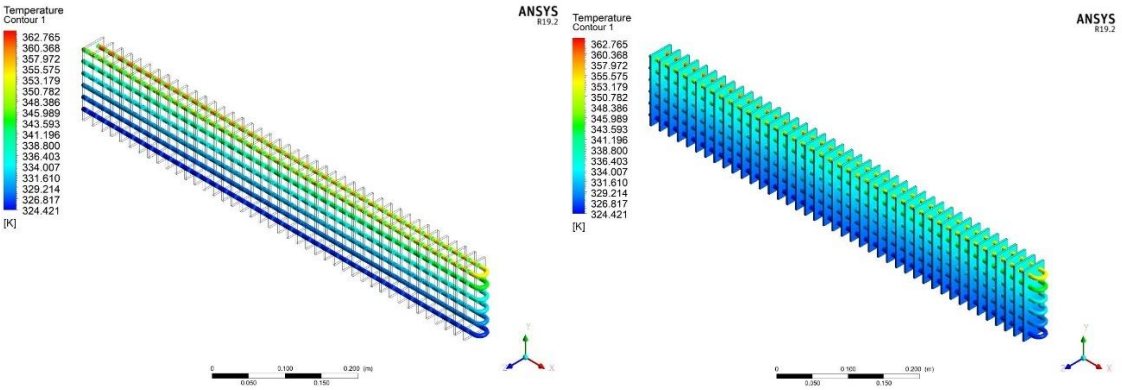

Fig. 7.8 Temperature contour of fin and tube condenser

Theoretical COP is found with the temperature and pressure readings and the corresponding enthalpy values.

$$\text{Theoretical COP, } (COP)_{Th} = \frac{h_1 - h_4}{h_2 - h_1} \quad (7.1)$$

Table 7.2 Results and COP for simulation of fin and tube condenser

Case	T_1	T_2	T_3	T_4	h_1	h_2	$h_3=h_4$	$(COP)_{th}$
	°C	°C	°C	°C	kJ/kg	kJ/kg	kJ/kg	
1	13.4	90.8	31.12	9.2	425	470	237.3	4.11
2	18.4	88.4	31.39	13.2	428	470	237.2	4.31
3	14.1	92.6	31.48	10.9	425	464	237.4	4.31
4	14.3	92.1	31.46	9.3	424	468	237.3	4.09
5	14.2	94.9	31.52	5.9	420	460	237.4	4.26
6	12.9	88.3	31.37	6.3	424	465	237.1	4.36

7.1.4 Simulation of Microchannel Condenser

Simulation of fluid flow through the microchannel condenser is also simulated with ANSYS Fluent. The temperature contour for flow of R22 through the microchannel condenser is shown in Fig. 7.9. From the temperature contour, it is evident that the temperature of R22 drops to temperature which almost equals the temperature of surrounding atmosphere. So, like all other cross flow heat exchangers, surrounding temperature is a vital factor in determining the outlet temperature. The temperature variation along at the middle of the cross section along the channel is shown in Fig. 7.10 and 7.11 and it also shows that the temperature drops rapidly at the inlet and remains almost constant near the outlet.

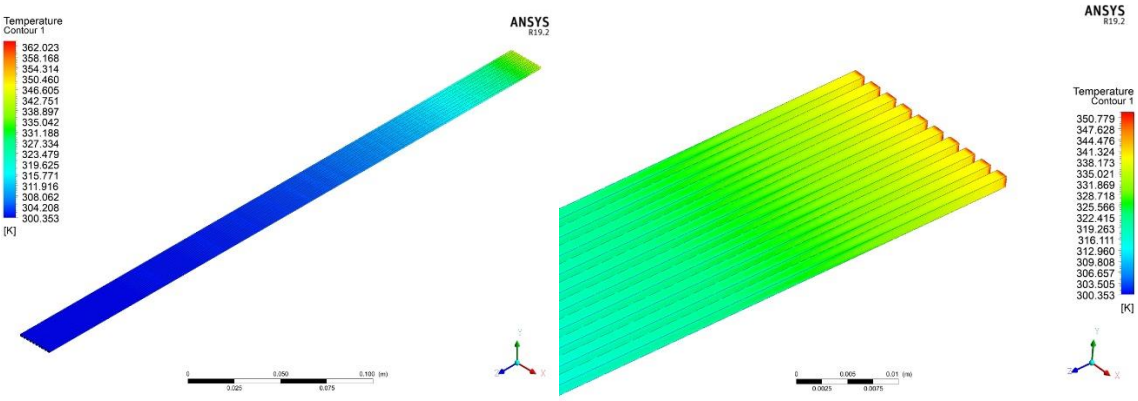

Fig. 7.9 Temperature contour for microchannel condenser

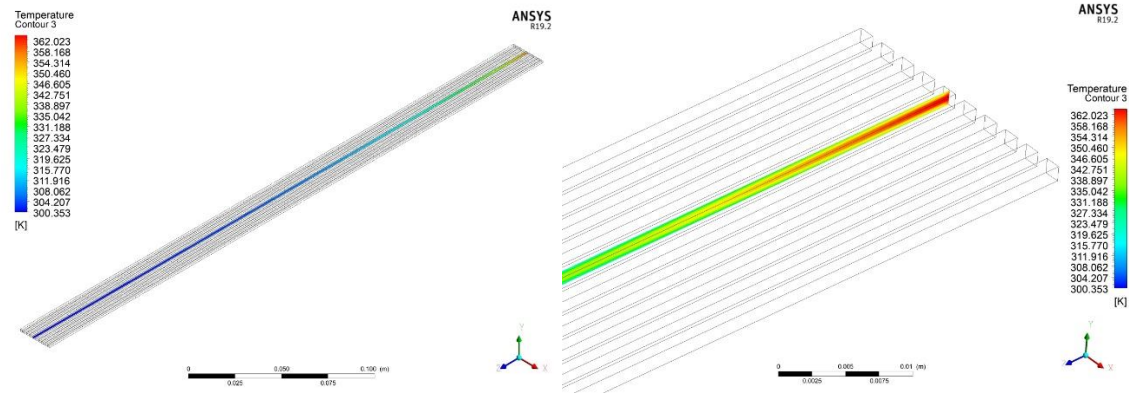

Fig. 7.10 Temperature variation at the middle of the channel

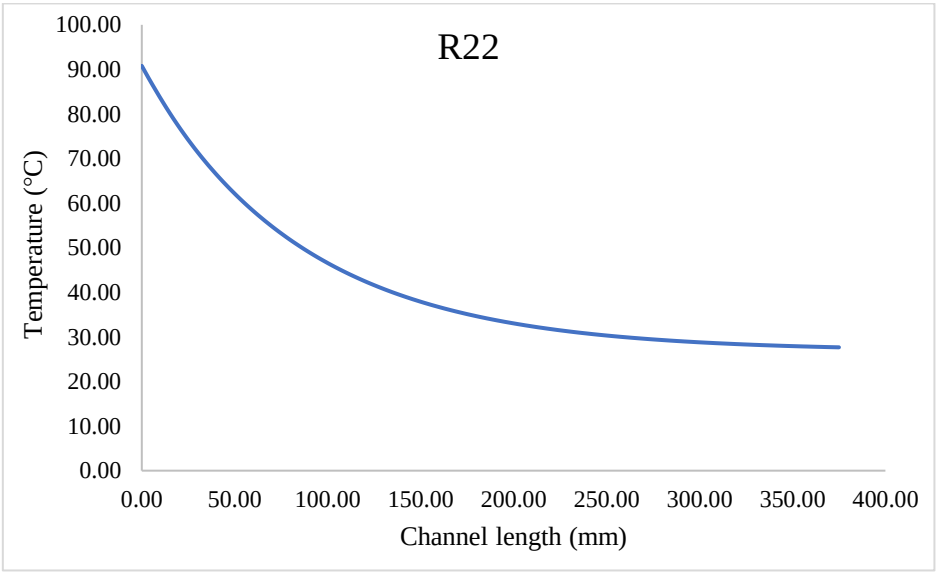

Fig 7.11 Temperature variation along the microchannel

The rapid drop in the temperature along the channel is due to the channel's cross section of micro dimensions. Small dimension cross section influences in improved heat transfer coefficient, thus effects in heat transfer and eventually faster temperature drop.

The temperature values, calculated coefficient of performance and the corresponding specific enthalpy values for the microchannel condenser are tabulated in Table 7.3.

Table 7.3 Results and COP for simulation of microchannel condenser

Case	T_1	T_2	T_3	T_4	h_1	h_2	$h_3=h_4$	$(COP)_{th}$
	°C	°C	°C	°C	kJ/kg	kJ/kg	kJ/kg	
1	13.4	90.8	26.89	9.2	425	470	233.61	4.25
2	18.4	88.4	26.86	13.2	428	470	233.58	4.63
3	14.1	92.6	27.92	10.9	425	464	234.90	4.87
4	14.3	92.1	26.90	9.3	424	468	233.63	4.33
5	14.2	94.9	27.98	5.9	420	460	234.98	4.63
6	12.9	88.3	26.86	6.3	424	465	233.58	4.64

7.1.5 Comparison of Simulation Results

Since the measured value of low pressure and high pressure of the system are 2 bar and 12 bar respectively, the Carnot COP value calculation is done with the corresponding saturation temperature values. The Carnot COP is given by:

$$(COP)_{Carnot} = \frac{T_L}{T_H - T_L} \tag{7.2}$$

Comparison of theoretical coefficient of performance for both the cases i.e., with fin and tube condenser and with microchannel condenser along with the corresponding Carnot COP is shown in Table 7.4.

Table 7.4 Comparison of simulation results

Case	Carnot COP	$(COP)_{th}$ with fin and tube condenser	$(COP)_{th}$ with microchannel condenser
1	5.28	4.11	4.25
2	5.28	4.31	4.63
3	5.28	4.31	4.87
4	5.28	4.09	4.33
5	5.28	4.26	4.63
6	5.28	4.36	4.64

From the comparison, it is clear that, COP is increases when microchannel condenser is employed. Graphical representation of the comparison is shown in Fig. 7.12.

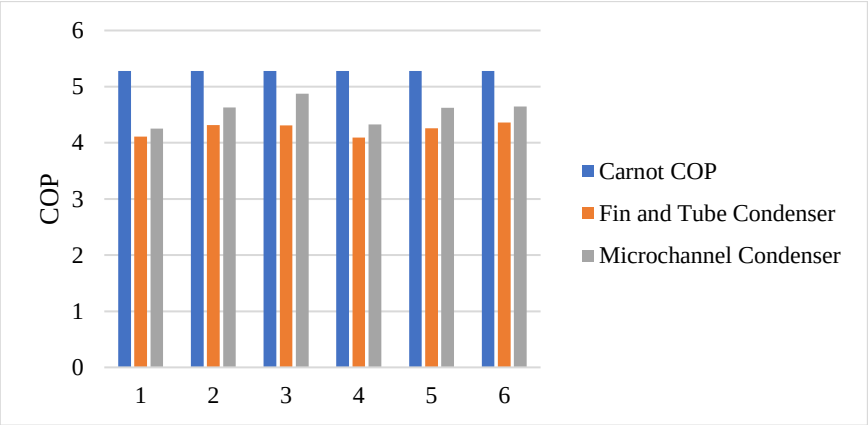

Fig. 7.12 Comparison of COP

The results from simulation shows that the COP can be improved up to 13% by using a microchannel condenser. Since only temperature and coefficient of performance is taken for consideration, another major benefit of the microchannel condenser, reduction in refrigerant charge is not calculated with the simulation.

7.2 EXPERIMENTAL RESULTS

7.2.1 Performance Analysis of Air Conditioning System

A residential split air conditioning system of capacity 2 TR using copper fin and tube condenser with refrigerant R22 is used for the experiment. Theoretical COP is calculated from the specific enthalpy values by plotting measured pressure and temperature values on the pressure-enthalpy chart of R22. For calculating actual COP, enthalpy values are taken from the psychrometric chart by plotting initial and final temperature (DBT) and relative humidity (RH). The power consumption of compressor is calculated from the voltage and current readings measured with multimeter.

Comparison of Carnot COP, theoretical COP and actual COP is shown in Fig. 7.6.

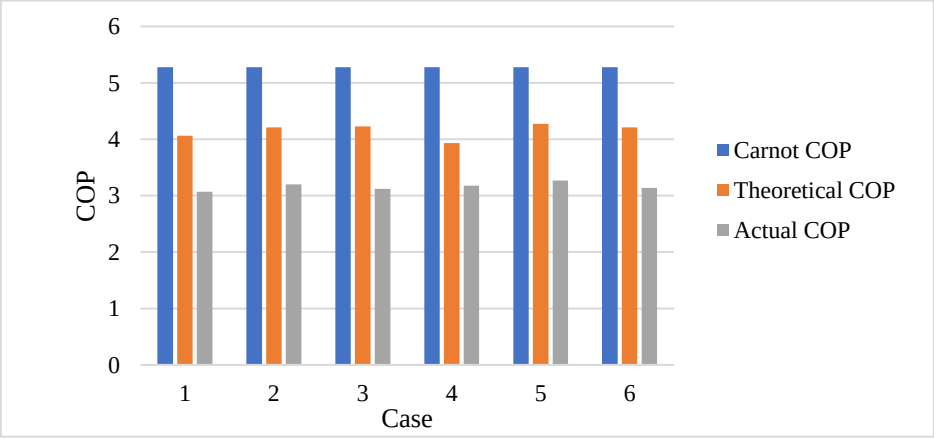

Fig. 7.13 Comparison of COP with fin and tube condenser

Table 7.5 Performance of the system with fin and tube condenser

Case	Initial Temperature	Initial Relative Humidity	Final Temperature	Final Relative Humidity	Thermocouple Readings				Pressure Readings		Theoretical COP	Actual COP
	DBT_i	RH_i	DBT_f	RH_f	T_1	T_2	T_3	T_4	LP	HP	$(COP)_{th}$	$(COP)_{actual}$
	°C	%	°C	%	°C	°C	°C	°C	bar	Bar		
1	26.8	81.9	24.6	66.3	13.4	90.8	40.5	9.2	2	12	4.06	3.07
2	27.3	84.9	22.4	81.6	18.4	88.4	40.2	13.2	2	12	4.21	3.2
3	27.6	84.8	20.2	76.9	14.1	92.6	41.4	10.9	2	12	4.23	3.12
4	33.8	66.1	25.4	67.2	14.3	92.1	41.9	9.3	2	12	3.93	3.18
5	35.6	57.8	24.8	62.7	14.2	94.9	42.9	5.9	2	12	4.27	3.27
6	32.3	68.3	24.9	63.8	12.9	88.3	42.4	6.3	2	12	4.21	3.14

Table 7.5 Performance of the system with fin and tube condenser

Case	Specific Enthalpy			Mass flow rate	Heat duty
	h_1	h_2	$h_3=h_4$	$\dot{m}$	$Q= \dot{m}(h_1-h_2)$
	kJ/kg	kJ/kg	kJ/kg	kg/s	Kw
1	425	470	250	0.04	9.7
2	428	470	251	0.05	10.3
3	425	464	252	0.05	10.8
4	424	468	251	0.05	9.8
5	420	460	249	0.05	10.4
6	424	465	251	0.05	10.3

7.3 TESTING OF MICROCHANNEL CONDENSER

The heat duty of microchannel condenser is checked with water before installing the condenser in the air conditioning system. Hot water is passed at the inlet of the heat exchanger and the outlet temperature is measured. Heat duty can be calculated from the mass flow rate and the temperature difference. The heat duty for the condenser can be calculated from the equation:

$$Q = \dot{m} c_p \Delta T = \dot{m} c_p (T_o - T_i) \quad (7.3)$$

Where c_p is the specific heat capacity. For water, c_p= 4.18 kJ/kgK.

The heat duty of the condenser is calculated by CFD simulation as well as with actual experiment.

7.3.1 Numerical Analysis

Like all other simulations mentioned in this study, ANSYS Fluent is used for the simulation of flow of water through the microchannel condenser to calculate the heat duty of the condenser. The inlet boundary condition is specified by the inlet mass flow rate and temperature of water. Temperature at both the boundaries are considered for heat duty calculation as per equation 7.3.

The temperature contour for flow of water through the microchannel condenser is shown in Fig. 7.14 and temperature variation at the middle of the channel is shown in Fig. 7.15 and 7.16.

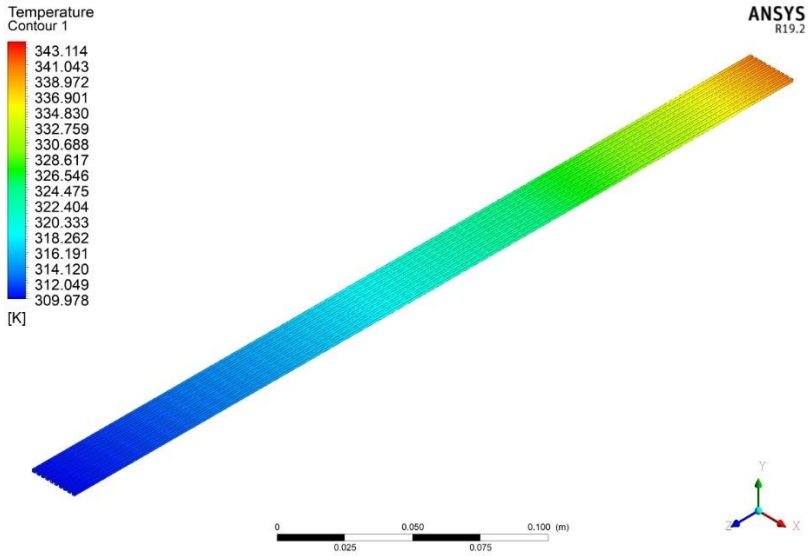

Fig. 7.14 Temperature contour for microchannel condenser with water

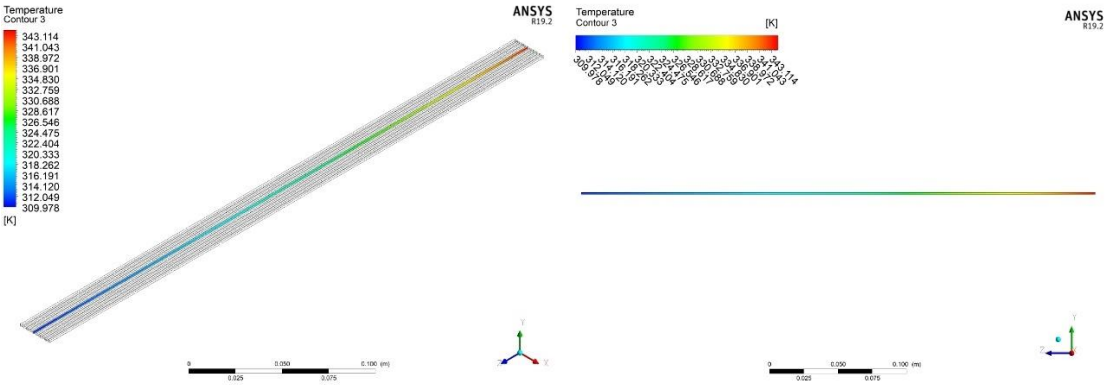

Fig. 7.15 Temperature variation at the middle of the channel for water

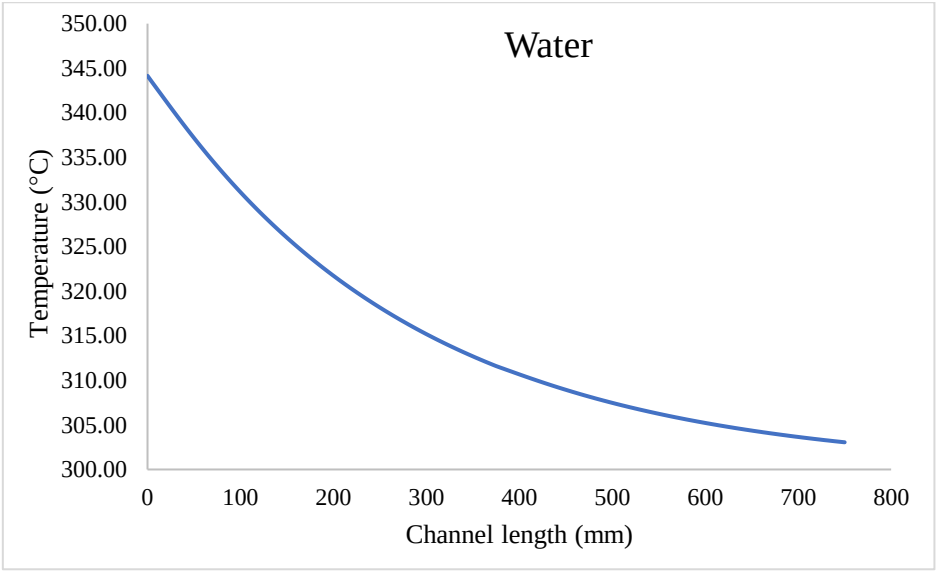

Fig 7.16 Temperature variation of water along the microchannel

The calculation of heat duty for the condenser with the temperature readings from the simulation are tabulated in Table 7.6

Table 7.6 Heat duty calculation with results from simulation

Sl No.	Mass flow rate	Inlet temperature	Outlet temperature	Heat duty
	$\dot{m}$	T_i	T_o	$Q= \dot{m}c_p\Delta T$
	kg/s	°C	°C	kW
1	0.132	60	26.97	18.22
2	0.177	59	27.31	23.45
3	0.167	62	27.26	24.25
4	0.175	63	27.37	26.06
5	0.178	60	27.36	24.29
6	0.027	71	26.84	12.37

7.3.2 Experiment

Measurement of temperature of water and heat duty calculation is done using an actual experiment set up also. Heat duty calculation for natural convection as well as for forced convection for the microchannel condenser is shown in Table 7.7 and 7.8 respectively. Infrared image of the condenser during both the cases are shown in Fig. 7.17.

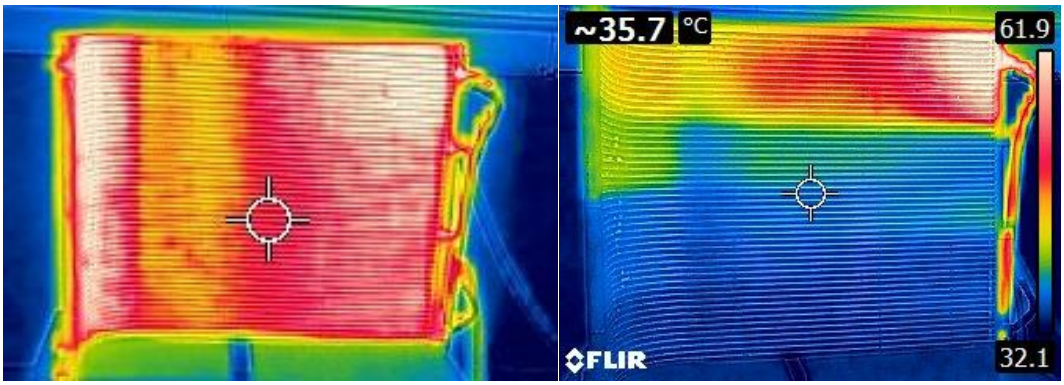

(a) Natural convection (b) Forced convection

Fig. 7.17 Infrared image of the condenser

Table 7.7 Heat duty calculation for natural convection

Sl No.	Mass flow rate	Inlet temperature	Outlet temperature	Heat duty
	$\dot{m}$	T_i	T_o	$Q= \dot{m}c_p\Delta T$
	kg/s	°C	°C	kW
1	0.132	60	54	3.31
2	0.177	59	51	5.92
3	0.167	62	54	5.58
4	0.175	63	56	5.12
5	0.178	60	51	6.70
6	0.027	71	53	2.03

Forced convection is provided on the condenser surface with a fan and as shown in Table 7.8. With forced convection, then temperature difference as well as the heat removed from the condenser is increased. The heat duty calculation gives satisfactory results when compared with the heat removed with a fin and tube condenser. So, the fin and tube condenser can be replaced with the microchannel condenser.

Table 7.8 Heat duty calculation for forced convection

Sl No.	Mass flow rate	Inlet temperature	Outlet temperature	Heat duty
	$\dot{m}$	T_i	T_o	$Q= \dot{m}c_p\Delta T$
	kg/s	°C	°C	kW
1	0.132	60	33	14.90
2	0.177	59	32	19.98
3	0.167	62	32	20.94
4	0.175	63	31	23.41
5	0.178	60	31	21.58
6	0.067	71	31	11.20

7.4 COMPARISON OF NUMERICAL AND EXPERIMENTAL RESULTS

Since the experiment and simulation are done with similar conditions, comparison can be done.

7.4.1 Fin and Tube Condenser

Comparison of COPs for the system with fin and tube condenser obtained from the numerical analysis and experiment is shown in Table 7.9 and Fig. 7.18.

Table 7.9 COP of the system with fin and tube condenser

Case	Coefficient of Performance (COP)	
	Experiment	Simulation
1	4.06	4.25
2	4.21	4.63
3	4.23	4.87
4	4.00	4.33
5	4.21	4.63
6	4.28	4.64

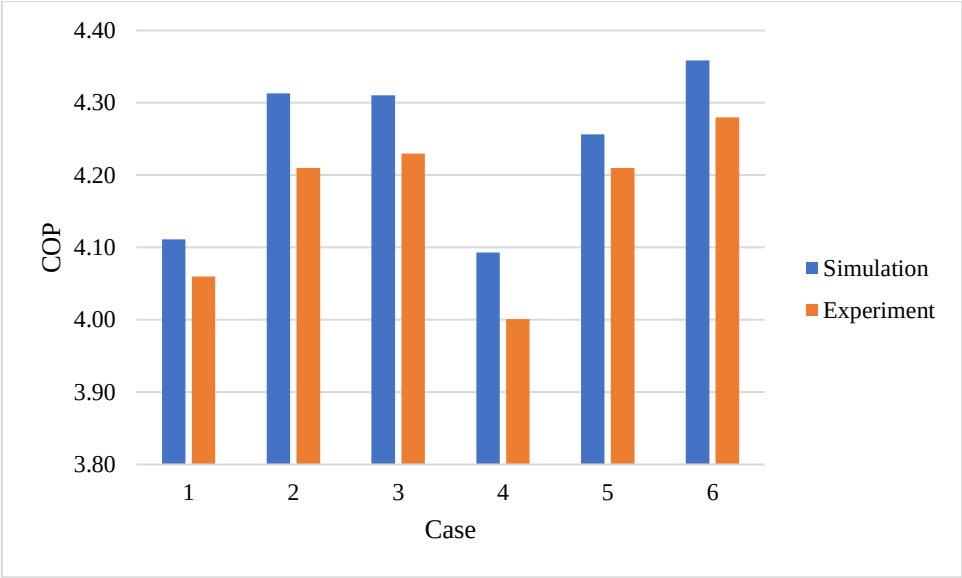

Fig. 7.18 COP of the system with fin and tube condenser

7.4.2 Microchannel Condenser

The amount of heat removed with the microchannel condenser, calculated from numerical analysis and experimental results are shown in Table 7.10 and their comparison is done in Fig. 7.19.

Table 7.10 Comparison of heat duty

Sl No.	Mass flow rate	Heat duty	
		Simulation	Experiment
	kg/s	kW	kW
1	0.067	12.37	11.20
2	0.132	18.22	14.90
3	0.167	24.25	20.94
4	0.175	26.06	23.41
5	0.177	23.45	19.98
6	0.178	24.29	21.58

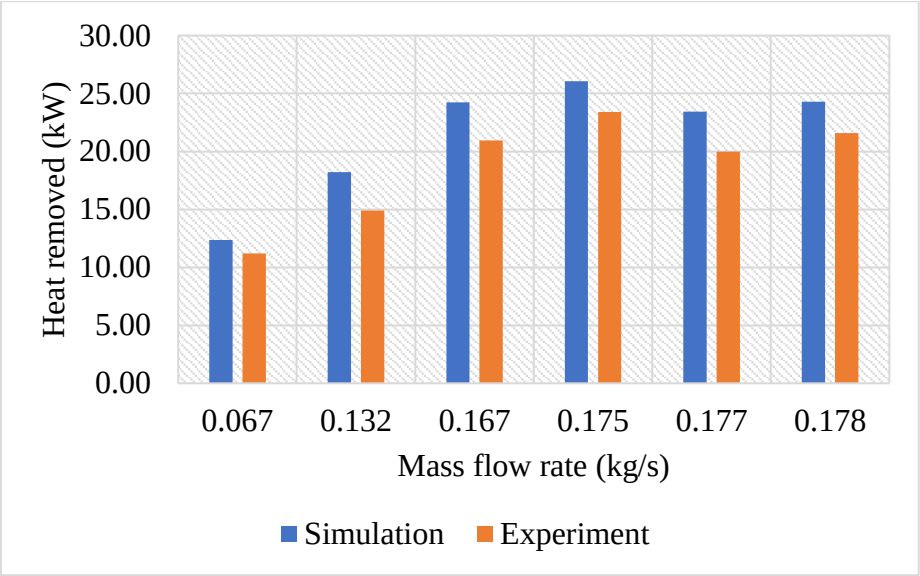

Fig. 7.19 Comparison of heat duty with simulation and experimental results

Coefficient of performance for the system with different cases are tabulated in Table 7.11

Table 7.11 Performance comparison of the system

Case		COP with fin and tube condenser		With microchannel condenser
	Carnot COP	Simulation	Experiment	Simulation
1	5.28	4.11	4.06	4.25
2	5.28	4.31	4.21	4.63
3	5.28	4.31	4.23	4.87
4	5.28	4.09	4.00	4.53
5	5.28	4.26	4.21	4.63
6	5.28	4.36	4.28	4.64

COP calculation on the *p-h* chart of R22 with both condensers is shown in Fig. 7.20. Subcooling with the microchannel condenser is one reason for improvement in COP. Graphical representation of the performance comparison of the system with both the condensers are shown in Fig 7.21.

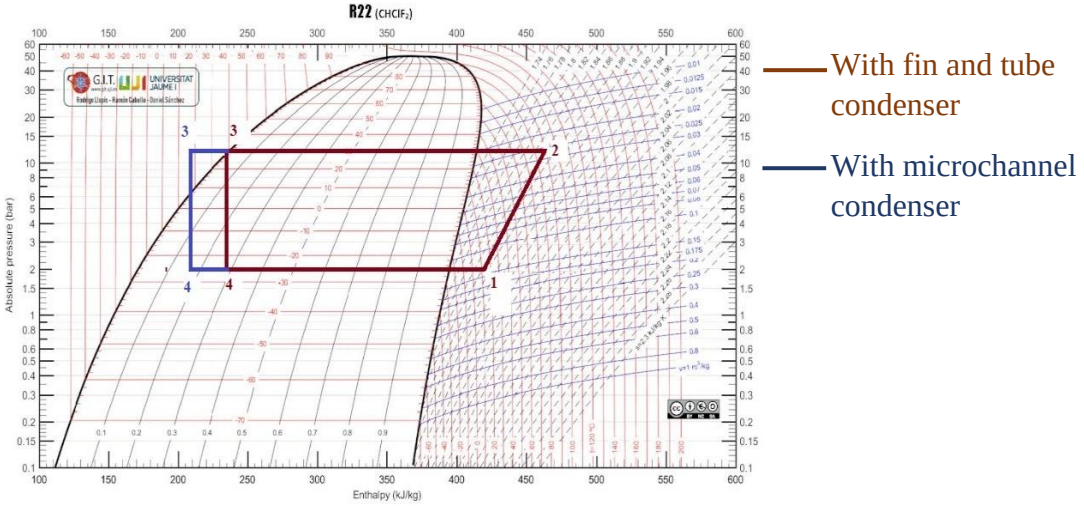

Fig. 7.20 COP calculation

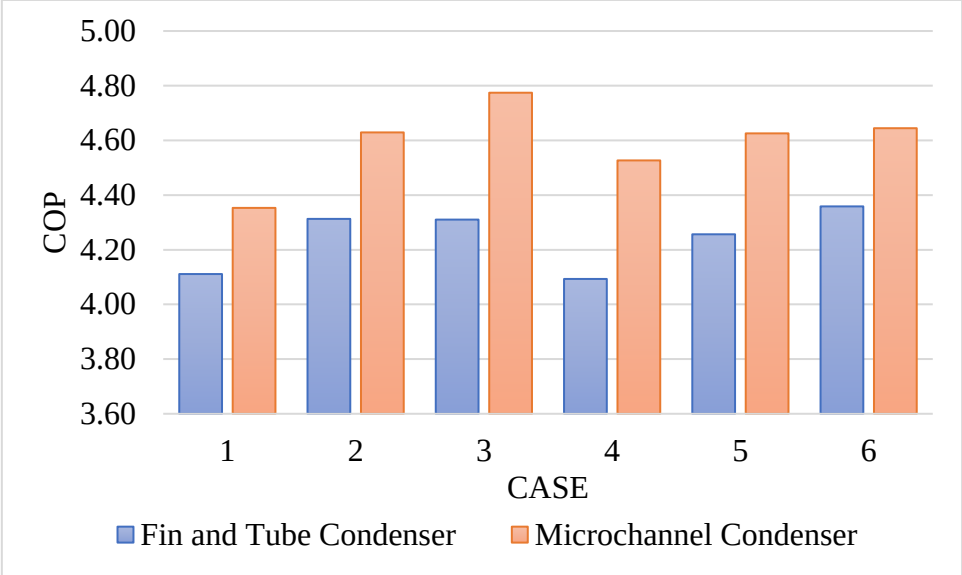

Fig. 7.21 Performance comparison with both condensers

CHAPTER 8: CONCLUSIONS AND SCOPE FOR FUTURE

8.1 CONCLUSIONS

In this research, refrigerant flow through microchannel is analysed and improvement in coefficient of performance of a residential split air conditioning system with a microchannel condenser is also studied. Using the CFD simulation, we find that the temperature of fluid flow in channel responses more quickly when the inlet area of channel becomes smaller resulting in the stronger heat transfer ability for micro-sized channels. More heat transfer area per unit volume provides another path to prove the enhancement in the heat transfer using small radii channel.

Initially, compatibility of the microchannel condenser with the air conditioning system is tested by calculating the heat duty of the condenser and comparing it with the fin and tube condenser. Both simulation and experimental results shows satisfactory results for the heat duty calculation. On an average, 82% improvement in heat duty was achieved with the microchannel condenser.

Performance enhancement of a residential split air conditioning system by replacing the fin and tube condenser with a microchannel condenser is studied using numerical simulation and the results were verified with the experimental data. With numerical analysis, an average of 10% and maximum 16% improvement in COP was achieved with the microchannel condenser.

Since the microchannel condenser is compact and lighter than the fin and tube condenser (38% reduction in weight), the fin and tube condenser can be successfully replaced with a microchannel condenser for performance enhancement.

8.2 FUTURE PROSPECTS

- Analysis of pressure drop across the microchannel condenser can be done and its influence on the system performance can be studied.
- Variation of system performance with variation in shape and dimensions of the microchannel can be studied.

REFERENCES

Aljubury, I. M. A. and Mohammed, M. A. (**2019**). Heat Transfer Analysis of Conventional Round Tube and Microchannel Condensers in Automotive Air Conditioning System. *Journal of Engineering*, *25*(2), 38–56.

Ansys, I. (**2020**). Ansys fluent theory guide; Ansys. *Inc*: *Canonsburg, PA, USA*

Basaran, A., Cemal Benim, A. and Yurddas, A. (**2019**). Prediction of heat and fluid flow in microchannel condensation. *E3S Web of Conferences*, 128, 01015.

Chen, Y., Hua, N. and Deng, L. S. (**2012**). Performances of a split-type air conditioner employing a condenser with liquid–vapor separation baffles. *International Journal of Refrigeration*, 35(2), 278–289.

Chen, X., Chen, Y., Deng, L., Mo, S., and Zhang, H. (**2013**). Experimental verification of a condenser with liquid–vapor separation in an air conditioning system. *Applied Thermal Engineering*, 51(1-2), 48–54.

Fung, C. K. and Majnis, M. F. (**2020**). Computational Fluid Dynamic Simulation Analysis of Effect of Microchannel Geometry on Thermal and Hydraulic Performances of Micro Channel Heat Exchanger. *Journal of Advanced Research in Fluid Mechanics and Thermal Sciences*, 62(2), 198–208.

Ganapathy, H., Shooshtari, A., Choo, K., Dessiatoun, S., Alshehhi, M. and Ohadi, M. M. (**2012**). Numerical Analysis of Condensation of R134a in a Single Microchannel. *International Mechanical Engineering Congress & Exposition.*

Goswami, M. K. and Babu, M. (**2019**). CFD and Thermal Analysis on AC Condenser by Using Different Fluids and Different Material. *International Journal for Recent Development in Science and Technology*. 3(12), 181-188.

Han, Y., Liu, Y., Li, M., and Huang, J. (**2012**). A review of development of micro-channel heat exchanger applied in air-conditioning system. *Energy Procedia*, 14, 148–153.

Harun-Or-Rashid, M. and Jeong, J. H. (**2018**). Replacement of Present Conventional Condenser of Household Refrigerator by Louver Fin Micro-Channel Condenser. *Arabian Journal for Science and Engineering*.

Hundy, G. F., Trott, A. R. and Welch, T. C. (**2016**). *Condensers and Cooling Towers.* Refrigeration, Air Conditioning and Heat Pumps, 99–120.

Illán-Gomez, F., García-Cascales, J.R., Hidalgo-Mompeán, F. and Lopez-Belchi, A. (**2017**). Experimental assessment of the replacement of a conventional fin-and-tube condenser by a minichannel heat exchanger in an air/water chiller for residential air conditioning. *Energy and Buildings*, 144, 104-116.

Kandlikar, S. G. and Grande, W. J. (**2003**). Evolution of Microchannel Flow Passages--Thermohydraulic Performance and Fabrication Technology. *Heat Transfer Engineering*, 24(1), 3–17.

Kim, M.-H. and Bullard, C. W. (**2002**). Performance Evaluation of a Window Room Air Conditioner with Microchannel Condensers. *Journal of Energy Resources Technology*, 124(1), 47.

Li, J. and Hrnjak, P. (**2017**). Separation in condensers as a way to improve efficiency, *International Journal of Refrigeration*, 79, 1-9.

Mehendale, S. (**2013**). Principles of Refrigerant Circuiting in Single Row Microchannel Evaporators. *ASME 2013 11th International Conference on Nanochannels, Microchannels, and Minichannels*.

Meral, Z. K. and Parlak, N. (**2021**). Experimental Research and CFD Simulation of Cross Flow Microchannel Heat Exchanger. *Journal of Thermal Engineering*, 7(2), 270-283.

Nagarjuna, V. and Srinivas, V. (**2021**). Study on heat transfer analysis of AC condenser by varying materials and refrigerants. *International Journal of Advance Research, Ideas and Innovations in Technology*, 7(4), 1282-1291.

Ohadi, M., Choo, K., Dessiatoun, S. and Cetegen, E. (**2012**). *Fundamentals of Microchannels*. SpringerBriefs in Applied Sciences and Technology.

Park, C. Y. and Hrnjak, P. S. (**2002**) R-410A Air Conditioning System With Microchannel Condenser. *International Refrigeration and Air Conditioning Conference*, 556.

Park, C. Y. and Hrnjak, P. (**2008**). Experimental and numerical study on microchannel and round-tube condensers in a R410A residential air-conditioning system. *International Journal of Refrigeration*, 31(5), 822–831.

Patil, D.P., Bhangale, J. H. and Deshmukh, K. S. (**2014**). Experimental Analysis of Refrigeration system using Micro channel condenser & Round Tube condenser. *International Journal of Innovative Research in Advanced Engineering*, 1(5), 192-198.

Ramesh, K. N., Sharma, T. K., and Rao, G. A. P. (**2020**). Latest Advancements in Heat Transfer Enhancement in the Micro-channel Heat Sinks: A Review. *Archives of Computational Methods in Engineering*, 28(4), 3135–3165.

Sachdeva R. C. (**2012**). *Fundamentals of Engineering Heat and Mass Transfer*, 4th edition, New Age International (P) Ltd.

Tuckerman, D. B. and Pease, R. F. W. (**1981**). High-performance heat sinking for VLSI. *IEEE Electron Device Letters*, 2(5), 126–129.

Wu, J., Wang, S. and Ge, Y. (**2009**). Experimental Research on Microchannel Heat Exchanger Performance for Residential Air Conditioner Applications. *ASME 2009 Second International Conference on Micro/Nanoscale Heat and Mass Transfer*, 3, 1-5.

Xia, L. and Chan, Y. (**2015**). Investigation of the Enhancement Effect of Heat Transfer Using Micro Channel. *Energy Procedia*, 75, 912–918.

Yin, X. W., Wang, W., Patnaik, V., Zhou, J. S., and Huang, X. C. (**2015**). Evaluation of microchannel condenser characteristics by numerical simulation. *International Journal of Refrigeration*, 54, 126–141.

Yun, R., Hwang, Y., Radermacher, R. and Zecirovic, R. (**2006**). Comparison of Performance of a Residential Air- Conditioning System Using Microchannel and Fin-and-Tube Heat Exchanger. *International Refrigeration and Air Conditioning Conference*, R108, 1-8.

Zanetti, E., Azzolin, M., Bortolin, S., Busato, G. and Col, D. D. (**2018**). Design And Testing of a Microchannel Heat Exchanger Working as Condenser and Evaporator. *International Refrigeration and Air Conditioning Conference*, 2593, 1-10.

Zhong, T., Chen, Y., Hua, N., Zheng, W., Luo, X., and Mo, S. (**2014**). In-tube performance evaluation of an air-cooled condenser with liquid–vapor separator. *Applied Energy*, 136, 968-978.

Zhou, J., Cao, X., Zhang, N., Yuan, Y., Zhao, X. and Hardy, D. (**2020**). Micro-Channel Heat Sink: A Review. *Journal of Thermal Science,* 29(6), 1431–1462.